Article

Not peer-reviewed version

Deriving the Born Rule from Boundary–Induced Alignment in Chronon Field Theory

Bin Li *

Posted Date: 28 August 2025

doi: 10.20944/preprints202508.2056.v1

Keywords: born rule; chronon field theory; stochastic processes; hydrodynamic limit; large deviations; Sanov's theorem; quantum foundation

 doi:10.20944/preprints202508.2056.v1

Article

Deriving the Born Rule from Boundary–Induced Alignment in Chronon Field Theory

Bin Li †

Research Department, Silicon Minds Inc.; binli.siliconminds@gmail.com
† Current address: Clarksville, MD, USA

Abstract

We derive the Born rule in Chronon Field Theory (ChFT) from first principles under realistic measurement assumptions. A recent work in ChFT shows that Lorentzian signature and causal structure emerge dynamically from a unit–norm constraint on the chronon field, providing the geometric foundation for the time–asymmetric alignment dynamics studied here. First, we obtain a diffusion limit for alignment order parameters on the outcome simplex and prove that the overlaps with apparatus eigen–domains form martingales up to the absorption time; optional stopping then yields single–shot Born probabilities. Second, we derive the stochastic limit from noisy chronon gradient flow with boundary coupling by a hydrodynamic limit (tightness, identification of the generator, and boundary layer analysis). Third, we establish a large–deviation principle for empirical frequencies in repeated measurements via Sanov's theorem, with rate function minimized at the Born vector. We quantify robustness to finite temperature, imperfect interfaces, and basis degeneracies, and outline falsifiable predictions for alignment timescales and drift bounds. Conceptually, the analysis shows that measurement is not a collapse of the system into one of its own eigenstates, but stochastic absorption of the system field into pre–stabilized apparatus eigen–domains. This does not directly contradict the standard textbook view—since apparatus domains are engineered to correspond to system eigenbases—but offers a deeper dynamical interpretation of why outcomes are definite and Born–weighted.

Keywords: born rule; chronon field theory; stochastic processes; hydrodynamic limit; large deviations; Sanov's theorem; quantum foundation

1. Introduction

Motivation.

Chronon Field Theory (ChFT) models quantum measurement as *boundary–induced alignment*, in which a microscopic chronon domain Ω with weakly correlated orientations couples across an interface Γ to a macroscopic apparatus region $\mathcal{A}$ whose coarse–grained field Φ^{μ}_{A} is stabilized (future–directed, unit–norm, twist–free). This coupling drives the domain's effective field Φ^{μ} into alignment with one of a finite set of apparatus eigen–domains, yielding a definite outcome without invoking nonlocal collapse. Prior work established that the Lorentzian, unit–norm phase is both exclusive and selected by measurement within apparatus regions, and showed that this phase emerges dynamically from a global unit–norm constraint on the chronon field in flat configuration space, thereby grounding causal structure and temporal asymmetry in the intrinsic geometry of the field space [63]. A key remaining challenge, and the focus of this paper, is to derive the *Born rule*—the quadratic dependence of outcome probabilities on initial amplitudes—from chronon dynamics alone, without introducing additional probabilistic axioms.

 doi:10.20944/preprints202508.2056.v1

Conceptual mechanism.

At the core of CFT is a field-theoretic model of quantum measurement in which outcome selection emerges from alignment geometry at the apparatus boundary. The apparatus defines a finite set of stabilized pointer configurations—the *eigen–domains*—with which the chronon field of the microscopic system can stochastically align. This alignment is local and continuous in spacetime, but due to coarse–graining and boundary coupling, the dynamics becomes probabilistic and irreversible on macroscopic scales. The outcome simplex encodes the overlaps between the evolving chronon field and these eigen–domains, and absorption into a vertex corresponds to a definite measurement result. Conceptually, this means that measurement is not a collapse of the system into one of its own eigenstates, but absorption of the system field into apparatus eigen–domains that are engineered to correspond to the system's eigenbasis. This does not contradict the standard textbook view, but reframes it: the apparatus, rather than the system, selects the effective measurement basis, yielding both outcome definiteness and Born weights from physical chronon dynamics without postulates.

Objective.

This paper provides an operational and rigorous derivation of the *Born rule* in the CFT measurement setting under explicit, verifiable assumptions on the apparatus, interface, and noise. That is, given a system prepared in state $|\psi\rangle$ and an observable with eigenstates $\{|a_i\rangle\}_{i=1}^m$, the probability of obtaining outcome a_i is

$$\Pr(a_i|\psi) = |\langle a_i|\psi\rangle|^2.$$

We treat the *alignment overlaps* with apparatus eigen–domains as order parameters,

$$p_i(t) \in [0,1], \qquad \sum_{i=1}^{m} p_i(t) = 1,$$

collectively forming a process on the outcome simplex Δ^{m-1}. Our main results establish that, under boundary–consistent noise and detailed balance at the interface, (i) the coarse–grained chronon dynamics yields a diffusion limit for $p(t)$ on Δ^{m-1} with absorbing vertices, (ii) the coordinates $p_i(t)$ are martingales up to the absorption time, and therefore (iii) single–shot absorption probabilities equal the initial overlaps $p_i(0)$, i.e., the Born weights. We then obtain a large–deviation principle (LDP) for empirical outcome frequencies in repeated trials, with rate function minimized at the Born vector.

Contributions.

In this paper we prove the following:

- **Geometric mechanism for outcome selection.** We model measurement as stochastic field alignment with a finite family of apparatus eigen–domains, yielding definite outcomes via absorption in the outcome simplex without invoking collapse.
- **Simplex diffusion (Theorem 3.1).** Starting from a noisy gradient–flow model for Φ with boundary coupling to Φ_A (consistent with a Gibbs noise model at inverse temperature β and interface strength η), we derive, under mild regularity and symmetry assumptions, a diffusion limit for the projected overlap process $p(t) = (p_1(t), \dots, p_m(t))$ on Δ^{m-1} with absorbing vertices $\{e_i\}_{i=1}^m$. The limiting generator has continuous, Lipschitz coefficients and preserves the simplex.
- **Martingale structure and Born probabilities (Proposition 17, Theorem 4.1).** We show that detailed balance at the interface enforces *zero drift* for each coordinate: $\mathbb{E}[\mathrm{d}p_i(t) \mid \mathcal{F}_t] = 0$. Hence $p_i(t)$ is a (uniformly integrable) martingale up to the absorption time τ at the simplex vertices. By optional stopping, the absorption probabilities satisfy

$$\mathbb{P}\big(p(\tau) = e_i\big) \;=\; \mathbb{E}\big[p_i(\tau)\big] \;=\; \mathbb{E}\big[p_i(0)\big] \;=\; p_i(0),$$

 doi:10.20944/preprints202508.2056.v1

yielding the Born rule when $p_i(0) = |c_i|^2$ are the initial overlaps with the apparatus eigen–domains.

- **Collapse as absorption (Section 5).** We interpret the selection of a definite measurement outcome as stochastic *absorption* of the alignment overlap vector $p(t)$ at a simplex vertex. This dynamical mechanism replaces the conventional wavefunction collapse postulate with a local, continuous, and probabilistic alignment process, reconciling definiteness of outcomes with causal and reversible dynamics.
- **Hydrodynamic grounding (Theorem 6.1).** We justify the diffusion approximation by proving tightness of the projected processes under chronon microdynamics, identifying the limit via the martingale problem [31], and computing the covariance from boundary fluctuations through a fluctuation–dissipation relation.
- **Frequency large deviations (Theorem 7.1).** For repeated measurements prepared with identical initial overlaps, we obtain a Sanov–type LDP for empirical frequencies $\hat{f}$ with good rate function $I(\hat{f}) = \sum_i \hat{f}_i \log(\hat{f}_i / p_i(0))$, minimized uniquely at $\hat{f}_i = p_i(0) = |c_i|^2$ [19].
- **Robustness bounds (Theorem 8.1).** We quantify deviations from Born weights under imperfect interfaces (finite η), finite temperature β^{-1}, and small symmetry–breaking drifts, obtaining explicit perturbative error bounds of the form $\left|\mathbb{P}_i - |c_i|^2\right| \leq C(\|\text{drift}\| + \eta^{-1/2} + \beta^{-1/2})$.

Relation to prior work.

Conceptually, our derivation parallels the martingale structure underlying stochastic Schrödinger equations and quantum trajectories [3,94], but differs in two essential ways: (i) the stochasticity arises from *classical* chronon fluctuations at the apparatus boundary within CFT's emergent causal geometry, rather than from postulated stochastic modifications to Schrödinger evolution; (ii) the simplex diffusion and its zero–drift property are derived from interface detailed balance and symmetry of the alignment energy, not imposed.

Compared to objective collapse models [6,39], our approach does not introduce new dynamical laws or coupling constants. Relative to purely epistemic accounts [13,84], outcome probabilities here emerge from physical stochastic absorption in the alignment geometry, not knowledge updates. Decoherence-based arguments [99] suppress interference but do not yield definite outcomes or derive Born weights; our model addresses both via the absorbing boundary structure of the outcome simplex.

Finally, unlike decision-theoretic derivations in Everettian settings [20,91], or subjectivist reconstructions such as QBism [34], the present framework grounds the Born rule in a local, emergent field theory with classical causal structure and no branching or agent-centric assumptions. The absorption law is tied directly to macroscopic alignment geometry and fluctuations, offering a new class of explanation distinct from stochastic mechanics [69] or gravitational collapse models [21,76].

Structure of the paper.

Section 2 formalizes the operational setting: apparatus eigen–domains, alignment overlaps, admissible noise, and observer axioms. Section 3 derives the limiting diffusion on the outcome simplex and states the required regularity and symmetry assumptions. Section 4 proves the martingale property and derives single–shot Born probabilities by optional stopping, including hitting and integrability lemmas. Section 6 provides the hydrodynamic limit from chronon microdynamics, establishing tightness and identifying the limiting generator and covariance via boundary fluctuation–dissipation. Section 7 proves the frequency LDP for repeated trials and sketches an alternative thermodynamic LDP via constrained free energies. Section 8 gives quantitative stability bounds and extensions to degeneracies and POVMs. Section 9 outlines experimental and numerical signatures. We conclude with a discussion of open problems and future directions.

To orient the reader, Figure 1 summarizes the logical pipeline/flowchart of our derivation. The starting point is the chronon dynamics in the apparatus boundary layer, modeled as a reversible noisy alignment process. Under suitable mixing and time–scale separation, these microscopic dynamics converge to an effective diffusion for the overlap vector on the outcome simplex. This diffusion is

 doi:10.20944/preprints202508.2056.v1

neutral and martingale–valued, so that absorption at the simplex vertices yields outcome probabilities equal to the initial overlaps—precisely the Born rule. At the level of repeated trials, empirical frequencies concentrate at the Born vector according to a large–deviation principle, providing a statistical law of large numbers with exponential accuracy. Finally, realistic imperfections such as finite coupling, temperature, or geometric asymmetry enter only as small drift or covariance corrections, for which quantitative stability bounds are available. In this way the figure provides a schematic overview, connecting microscopic chronon alignment to the emergence and robustness of Born statistics.

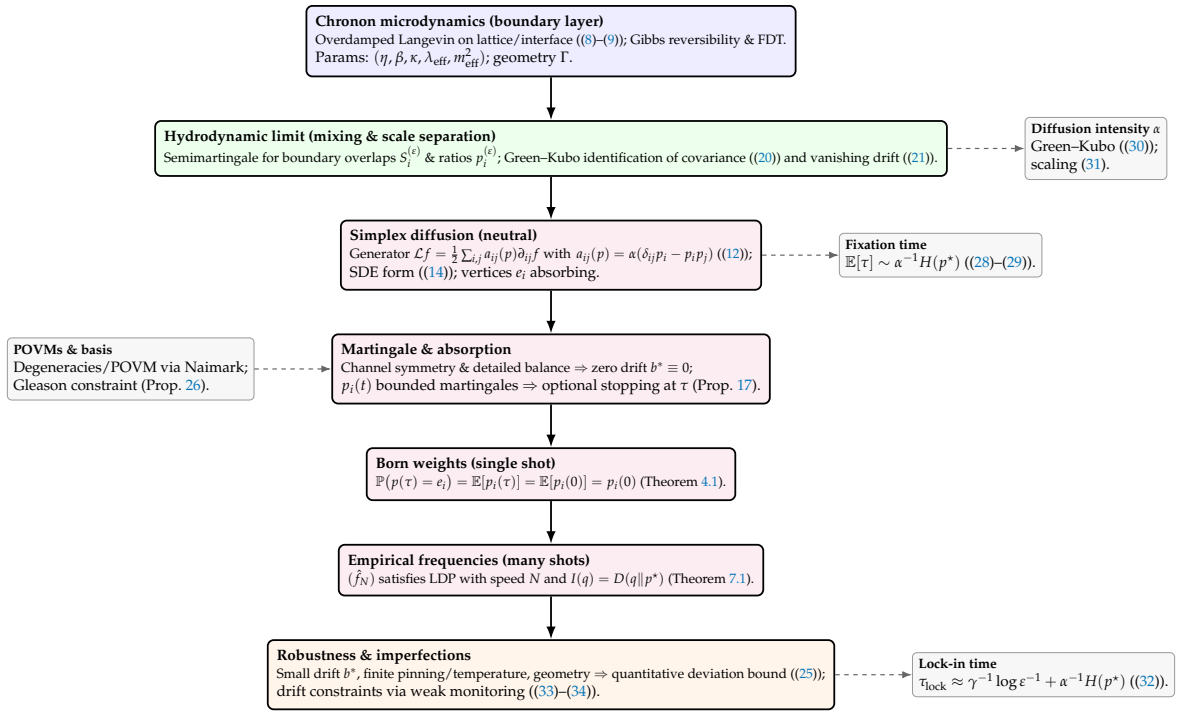

Figure 1. Pipeline from chronon microdynamics to observable outcome statistics. See Figure 1. Starting from microscopic "chronon" dynamics at the apparatus boundary, the system relaxes by reversible noisy alignment. In the hydrodynamic limit this reduces to a neutral Wright–Fisher diffusion for the overlap vector on the outcome simplex. Because each overlap coordinate is then a martingale, absorption at the simplex vertices yields outcome probabilities equal to the initial overlaps — the Born rule. Repeating the experiment many times, empirical frequencies concentrate at the Born vector with exponentially small deviations (Sanov LDP). Finite interface strength, temperature, or asymmetries only introduce small, quantifiable corrections.

For Non-specialists. Because some of our arguments draw on techniques from probability theory, statistical physics, and information theory, we provide a self-contained pedagogical appendix for non-specialist readers. There we review the essential background on martingales and optional stopping, Wright–Fisher diffusions on the simplex, and large deviations via relative entropy and Sanov's theorem, together with simple examples and diagrams. Readers familiar with these standard tools may skip the appendix.

2. Operational Setup and Measurement Geometry

2.1. Apparatus Eigen–Domains and Alignment Observables

We formalize the macroscopic apparatus, its stabilized alignment field, the measurement interface, and the outcome observables that will generate a process on the outcome simplex.

Definition 1 (Stabilized apparatus domain)**.** An *apparatus domain* is an open, connected subset $\mathrm{A} \subset M$ equipped with a smooth, future–directed, unit–norm timelike vector field

$$\Phi^\mu_{\mathrm{A}} \in \Gamma(T\mathrm{A}), \qquad g_{\mu\nu}\Phi^\mu_{\mathrm{A}}\Phi^\nu_{\mathrm{A}} \equiv -1, \qquad \Phi^0_{\mathrm{A}} > 0,$$

 doi:10.20944/preprints202508.2056.v1

that is *twist–free* in A:

$$\omega_{\mu\nu}[\Phi_{\mathrm{A}}] := h_{\mu}^{\ \alpha} h_{\nu}^{\ \beta} \nabla_{[\alpha} \Phi_{\mathrm{A},\beta]} \equiv 0, \qquad h_{\mu\nu} := g_{\mu\nu} + \Phi_{\mathrm{A},\mu} \Phi_{\mathrm{A},\nu}.$$

Consequently, there exists a smooth proper–time function τ on A whose level sets $\{\Sigma_\tau\}$ are spacelike hypersurfaces orthogonal to Φ_{A}^{μ}. We call $\{\Sigma_\tau\}$ the *apparatus foliation*.

Remark 2 (Emergent causal structure from chronon constraints). The apparatus field Φ_{A}^{μ} induces the local causal structure and time direction in A by defining a unit–norm, twist–free timelike flow. This structure is not imposed arbitrarily: in a companion analysis [63], it is shown that such Lorentzian signature arises naturally from a unit–norm constraint on the chronon field Φ^{μ} over a flat background configuration space. There, the kinetic term in the effective action, constrained to preserve unit norm, selects a hyperbolic geometry with a distinguished timelike direction—providing a geometric foundation for the causal alignment process assumed in the present derivation. (See Appendix L for a justification of the eigen–domain structure.)

Definition 3 (Measurement interface and channels)**.** Let $\Omega \subset M$ be the (mesoscopic) microdomain prepared for measurement, and let $\Gamma := \partial\Omega \cap \mathrm{A} \cap \Sigma_{\tau_0}$ be the spacelike measurement interface on a fixed apparatus leaf Σ_{τ_0}. Denote by γ the induced Riemannian metric on Γ and by $\mathrm{d}\sigma_\gamma$ its volume form.

A family of $m \in \mathbb{N}$ *channels* is a measurable partition

$$\Gamma = \bigsqcup_{i=1}^{m} \Gamma_i, \qquad \Gamma_i \cap \Gamma_j = \emptyset \ (i \neq j),$$

with each Γ_i of positive γ–measure. Define $u_i := \mathbf{1}_{\Gamma_i} / \|\mathbf{1}_{\Gamma_i}\|_{L^2(\Gamma,\mathrm{d}\sigma_\gamma)} \in L^2(\Gamma)$, so that

$$\langle u_i, u_j \rangle_{L^2(\Gamma)} = \delta_{ij}, \qquad \sum_{i=1}^{m} \langle \cdot, u_i \rangle u_i \text{ is the orthogonal projector onto } \operatorname{span}\{u_i\}.$$

We refer to $\{\Gamma_i\}$ (or $\{u_i\}$) as the *apparatus eigen–domains* (resp. an *orthonormal channel basis*).

Remark 4 (Geometry and physical meaning). The field Φ_{A}^{μ} fixes the local time direction and causal geometry in A (Def. 1). The partition $\{\Gamma_i\}$ encodes distinct, macroscopically disjoint pointer channels (e.g. separate detector pixels or paths) on the interface where the microdomain first couples to the apparatus. Orthogonality is in the *function space* $L^2(\Gamma)$, not in Minkowski space; distinct channels are disjoint in space, which is the operational origin of outcome exclusivity [98].

Remark 5 (Channel symmetry and standard QM). In the present framework, we assume symmetry of the apparatus eigen–domains, so that no outcome channel is intrinsically favored beyond the system's own overlaps. This assumption is not an additional hypothesis, but rather the field–theoretic restatement of what is already built into the standard measurement postulate: projective measurements treat all eigenstates of a given observable on equal footing, and more generally POVMs require $\sum_i E_i = I$, ensuring completeness and unbiasedness of the outcome channels. In textbook quantum mechanics this symmetry is taken as axiomatic, whereas here it is realized dynamically through the geometry and stochastic alignment of the apparatus domains.

Definition 6 (Alignment scalar and alignment observable)**.** Let Φ^{μ} be the coarse–grained chronon field in a neighbourhood of Γ. Define the *local alignment scalar* on Γ by

$$s(x) := -\, g_{\mu\nu}\, \Phi_{\mathrm{A}}^{\mu}(x)\, \Phi^{\nu}(x), \qquad x \in \Gamma,$$

 doi:10.20944/preprints202508.2056.v1

which satisfies $s(x) \geq 1$ whenever both Φ_A and Φ are unit–norm, future–directed timelike fields. Let $f : [1, \infty) \to [0, \infty)$ be a fixed C^1 strictly increasing function (e.g. $f(r) = r^2$). The *channel strengths* are

$$S_i(\Phi) := \int_\Gamma u_i(x)\, f\big(s(x)\big)\, \mathrm{d}\sigma_\gamma(x) \;=\; \int_{\Gamma_i} f\big(s(x)\big)\, \mathrm{d}\sigma_\gamma(x), \qquad i = 1, \ldots, m.$$

Definition 7 (Alignment overlaps and outcome simplex)**.** Provided $\sum_{j=1}^m S_j(\Phi) > 0$, define the *alignment overlaps* (or *overlap vector*)

$$p_i(\Phi) \;:=\; \frac{S_i(\Phi)}{\sum_{j=1}^m S_j(\Phi)}, \qquad i = 1, \ldots, m.$$

Then $p(\Phi) := (p_1(\Phi), \ldots, p_m(\Phi))$ takes values in the outcome simplex

$$\Delta^{m-1} \;:=\; \Big\{ p \in [0,1]^m \;:\; \sum_{i=1}^m p_i = 1 \Big\}.$$

Lemma 8 (Normalization, positivity, and continuity)**.** *Under the hypotheses of Definitions 1–7, the map $\Phi \mapsto p(\Phi)$ is well–defined on the set where $\sum_j S_j(\Phi) > 0$ and satisfies:*

1. $0 \leq p_i(\Phi) \leq 1$ *and* $\sum_i p_i(\Phi) = 1$.
2. *If $\Phi = \Phi_A$ on Γ, then $s(x) \equiv 1$, $S_i(\Phi) = \mathrm{Area}_\gamma(\Gamma_i)$, and hence $p_i(\Phi) = \mathrm{Area}_\gamma(\Gamma_i)/\mathrm{Area}_\gamma(\Gamma)$.*
3. *If Φ varies in H^1 in a neighbourhood of Γ, then $p(\Phi)$ depends continuously on Φ with respect to the H^1–topology (equivalently, continuously in $L^2(\Gamma)$ via the trace), provided f is C^1 with bounded derivative on bounded sets [9,32].*

Remark 9 (Choice of f and invariance). Any strictly increasing f yields the same *ordering* of channel strengths and, after normalization, the same $p(\Phi)$ up to a continuous, strictly order–preserving reparametrization of the pre–normalized scores. The choice $f(r) = r^2$ is convenient analytically (smooth, convex) and physically interpretable as a quadratic energy gain from alignment [37].

Remark 10 (Single–point vs. spatially averaged overlaps). The L^2 channel basis $\{u_i\}$ (Def. 3) implements a spatial coarse–graining of the local alignment scalar over each channel Γ_i. This averaging is essential for robustness and for the hydrodynamic limit: it ensures that $p(\Phi)$ is insensitive to microscopic fluctuations below the interface scale and provides Lipschitz continuity of the overlaps with respect to Φ in trace norms, which will be used in Sections 3–6 [85].

Dynamics notation.

In Sections 3–4 we write $p_i(t) := p_i(\Phi(\cdot, t))$ for the *time–dependent* overlaps induced by the (noisy) alignment dynamics of Φ near Γ. By Lemma 8, $p(t) \in \Delta^{m-1}$ for all times prior to absorption at a channel, and $p(t)$ will be shown to evolve as a diffusion on Δ^{m-1} with absorbing vertices under suitable assumptions.

2.2. Observer Axioms and Admissible Dynamics

We recall the operational axioms that constrain physically realizable observers and specify the admissible stochastic dynamics for the alignment process at the measurement interface. The axioms ensure causal consistency at the macroscopic level; the dynamics below is an effective description of boundary–driven relaxation in the apparatus and will be shown to imply a diffusion limit for the alignment overlaps on the outcome simplex.

Definition 11 (Observer axioms)**.** An *observer* is a macroscopic open system supported in a stabilized apparatus domain A (Definition 1) whose operation satisfies:

(O1) **Well–posed local dynamics.** The physical degrees of freedom (matter + fields) obey local second–order PDEs admitting a well–posed Cauchy problem on spacelike slices Σ_τ of the apparatus foliation [47].

 doi:10.20944/preprints202508.2056.v1

(O2) **Finite–speed signalling.** There exists a cone structure compatible with (A, g) such that disturbances from compactly supported initial data propagate inside the corresponding domains of dependence.
(O3) **Acyclic causal order.** The causal precedence relation on A is irreflexive and transitive; no closed causal loops exist in the operational regime.
(O4) **Records and stability.** There exist subsystems of finite spatial extent whose internal macrostates encode outcomes and remain metastable for times $\gg \tau_{\mathrm{dyn}}$, the microscopic relaxation scale [51,97].

Interface parameters.

We fix an apparatus leaf Σ_{τ_0} and a spacelike interface $\Gamma \subset \Sigma_{\tau_0}$ (Definition 3) with orthonormal channel basis $\{u_i\}_{i=1}^{m} \subset L^2(\Gamma)$. Two control parameters enter the interface model:

$$\eta > 0 \quad \text{(interface coupling strength)}, \qquad \beta > 0 \quad \text{(inverse temperature of the boundary bath)}.$$

The coupling η quantifies the energetic penalty for misalignment between Φ and Φ_{A} on Γ; the temperature β^{-1} parameterizes thermal fluctuations of the chronon degrees of freedom in the boundary layer.

Effective alignment functional.

On a neighbourhood U of Γ we consider the coarse–grained functional (bulk + boundary)

$$\mathcal{F}_\eta[\Phi] \;=\; \int_U \sqrt{|g|}\,\Big\{\tfrac{\kappa}{2}\nabla_\alpha\Phi^\mu\nabla^\alpha\Phi_\mu + \tfrac{m_{\mathrm{eff}}^2}{2}\Phi^\mu\Phi_\mu + \tfrac{\lambda_{\mathrm{eff}}}{4}(\Phi^\mu\Phi_\mu+1)^2\Big\} \;+\; \eta\int_\Gamma\sqrt{|\gamma|}\,\Big(1-\Phi\cdot\Phi_{\mathrm{A}}\Big)^2, \quad (1)$$

with $\kappa > 0$, $\lambda_{\mathrm{eff}} > 0$, $m_{\mathrm{eff}}^2 < 0$ (ordered phase).

Definition 12 (Admissible alignment dynamics)**.** An *admissible dynamics* for Φ near Γ is either of the following two classes:

(H) Hyperbolic (causal) stochastic dynamics. A damped stochastic wave equation on U,

$$\partial_t^2\Phi^\mu + \gamma\,\partial_t\Phi^\mu \;=\; -\frac{\delta\mathcal{F}_\eta}{\delta\Phi_\mu} \;+\; \sqrt{2\beta^{-1}}\,(\mathcal{M}_H^{1/2}\,\Xi)^\mu, \quad (2)$$

with $\gamma > 0$, where Ξ is a space–time Gaussian field of zero mean, white in time and smooth at spatial scale ξ_{b} (the boundary microscopic scale), and $\mathcal{M}_H$ is a positive self–adjoint mobility operator on U. Boundary condition on Γ:

$$\kappa\,\nabla_n\Phi^\mu + 2\eta\,(1-\Phi\cdot\Phi_{\mathrm{A}})\,\Phi_{\mathrm{A}}^\mu \;=\; \sqrt{2\beta^{-1}}\,(\mathcal{B}_H^{1/2}\,\zeta)^\mu, \quad (3)$$

with outward normal n, Gaussian boundary noise ζ (white in time, smooth on Γ), and positive self–adjoint boundary mobility $\mathcal{B}_H$.

(P) Overdamped (gradient–flow) stochastic dynamics. An L^2–gradient flow on U,

$$\partial_t\Phi^\mu \;=\; -\,(\mathcal{M}_P\,\delta\mathcal{F}_\eta/\delta\Phi)^\mu \;+\; \sqrt{2\beta^{-1}}\,(\mathcal{M}_P^{1/2}\,\Xi)^\mu, \quad (4)$$

with boundary condition

$$\kappa\,\nabla_n\Phi^\mu + 2\eta\,(1-\Phi\cdot\Phi_{\mathrm{A}})\,\Phi_{\mathrm{A}}^\mu \;=\; \sqrt{2\beta^{-1}}\,(\mathcal{B}_P^{1/2}\,\zeta)^\mu, \quad (5)$$

where $\mathcal{M}_P$ and $\mathcal{B}_P$ are positive self–adjoint mobilities (bulk and boundary).

 doi:10.20944/preprints202508.2056.v1

Assumption 13 (Detailed balance and fluctuation–dissipation)**.** In either class (H) or (P), the bulk and boundary mobilities $\mathcal{M}_\bullet, \mathcal{B}_\bullet$ are chosen so that the Markov semigroup of the process is *reversible* with respect to the Gibbs measure

$$\mu_{\beta,\eta}(\mathrm{d}\Phi) \;\propto\; \exp\big(-\beta\,\mathcal{F}_\eta[\Phi]\big)\,\mathrm{d}\Phi, \tag{6}$$

i.e. detailed balance holds:

$$\int F\,\mathcal{L}G\,\mathrm{d}\mu_{\beta,\eta} \;=\; \int G\,\mathcal{L}F\,\mathrm{d}\mu_{\beta,\eta} \qquad \text{for all smooth cylinder } F, G,$$

where $\mathcal{L}$ is the generator. Equivalently, the noise covariances satisfy the fluctuation–dissipation relation with the same mobilities that define the drift $-\mathcal{M}\nabla\mathcal{F}_\eta$ (class P) or the damping operators (class H).

Assumption 14 (Well–posedness and locality)**.** For class (H), the deterministic part of (2) is strictly hyperbolic with finite propagation speed in (U, g); the stochastic forcing Ξ, ζ has compact spatial correlation support of diameter $\le \xi_{\mathrm{b}}$, ensuring that for any $t > 0$ the influence of data outside the domain of dependence is exponentially suppressed. For class (P), the dynamics (4) is the overdamped limit of (H) on timescales $\gg \gamma^{-1}$; it is confined to a thin tubular neighbourhood of Γ of thickness $\mathcal{O}(\xi_{\mathrm{b}})$ and cannot be used operationally for signalling outside A. In both cases, for initial data $\Phi_0 \in H^1(U)$ there exists a unique (probabilistically strong) solution with continuous paths in H^1 on finite time intervals.

Remark 15 (Compatibility with observer axioms). Axioms (O1)–(O3) apply to the macroscopic propagation of matter and information in A. Class (H) respects finite–speed propagation at the level of alignment dynamics. Class (P) is an effective, strongly damped limit describing local relaxation of Φ inside the apparatus boundary layer; since it is confined to U and reversible w.r.t. $\mu_{\beta,\eta}$, it does not generate superluminal signalling or causal anomalies at the operational level. Axiom (O4) is ensured by the existence and uniqueness of the minimizer of $\mathcal{F}_\eta$ in the apparatus (stability of records), as established in the measurement selection results.

Consequence for overlaps.

Under Assumptions 13–14, the process $t \mapsto p(t) = p(\Phi(\cdot, t))$ (Definition 7) is a Markov process on Δ^{m-1} whose drift is determined by the $\mu_{\beta,\eta}$–reversible dynamics. In Section 3 we prove that, after a diffusive rescaling and projection, $p(t)$ converges to a diffusion with absorbing vertices and, by detailed balance, has *zero drift* along each coordinate—yielding the martingale structure central to our Born–rule derivation.

3. From Noisy Alignment Dynamics to a Simplex Diffusion

3.1. Noisy Gradient Flow for Φ with Boundary Coupling

We work with the overdamped (gradient–flow) class (P) from Definition 12, in the spirit of stochastic gradient flows for SPDEs [17]. Let U be a tubular neighbourhood of the interface $\Gamma \subset \Sigma_{\tau_0}$. The coarse–grained alignment functional is

$$\mathcal{F}_\eta[\Phi] \;=\; \int_U \sqrt{|g|}\,\Big\{\tfrac{\kappa}{2}\nabla_\alpha\Phi^\mu\nabla^\alpha\Phi_\mu + \tfrac{m_{\mathrm{eff}}^2}{2}\Phi^\mu\Phi_\mu + \tfrac{\lambda_{\mathrm{eff}}}{4}(\Phi^\mu\Phi_\mu + 1)^2\Big\} + \eta\int_\Gamma\sqrt{|\gamma|}\,\Big(1 - \Phi\cdot\Phi_{\mathrm{A}}\Big)^2, \tag{7}$$

with $\kappa > 0$, $\lambda_{\mathrm{eff}} > 0$, $m_{\mathrm{eff}}^2 < 0$ fixed.

The stochastic alignment dynamics is the L^2 gradient flow of $\mathcal{F}_\eta$ with Gibbs–consistent noise (Assumption 13), consistent with the fluctuation–dissipation framework for SPDEs [45,86]:

$$\mathrm{d}\Phi^\mu(t) = -\,(\mathcal{M}_P\,\delta\mathcal{F}_\eta/\delta\Phi)^\mu(\Phi(t))\,\mathrm{d}t \;+\; \sqrt{2\beta^{-1}}\,(\mathcal{M}_P^{1/2}\,\mathrm{d}W_t)^\mu \qquad \text{in } U, \tag{8}$$

$$\kappa\,\nabla_n\Phi^\mu(t)\big|_\Gamma + 2\eta\,(1 - \Phi\cdot\Phi_{\mathrm{A}})\,\Phi_{\mathrm{A}}^\mu\big|_\Gamma \;=\; \sqrt{2\beta^{-1}}\,(\mathcal{B}_P^{1/2}\,\mathrm{d}B_t)^\mu \qquad \text{on } \Gamma, \tag{9}$$

 doi:10.20944/preprints202508.2056.v1

where W is a cylindrical Wiener process on $L^2(U)$ with covariance trace–class at spatial scale ξ_b, B is a boundary Wiener process on $L^2(\Gamma)$ with trace–class covariance, and $\mathcal{M}_P$, $\mathcal{B}_P$ are positive self–adjoint mobilities. By Assumption 14, for any $\Phi_0 \in H^1(U)$, (8)–(9) has a unique strong solution with continuous H^1–paths on finite times [17].

Let $T : H^1(U) \to L^2(\Gamma)$ be the trace operator. Recall the *alignment overlaps* (Def. 7) built from the local scalar $s(x) = -g_{\mu\nu}\, \Phi_A^{\mu}(x)\, (T\Phi)^{\nu}(x)$ and a fixed strictly increasing $f \in C^1([1,\infty))$:

$$S_i(\Phi) := \int_{\Gamma_i} f(s(x))\, \mathrm{d}\sigma_\gamma(x), \qquad p_i(\Phi) := \frac{S_i(\Phi)}{\sum_{j=1}^m S_j(\Phi)}.$$

Set $p(t) := p(\Phi(t)) \in \Delta^{m-1}$.

To compute the stochastic evolution of $p(t)$ we use Itô's formula for functionals of infinite–dimensional diffusions [17]. If $F : H^1(U) \to \mathbb{R}$ is twice Fréchet differentiable with appropriate growth and trace–class noise, then

$$\begin{aligned} \mathrm{d}F(\Phi(t)) = DF(\Phi)\big[-\mathcal{M}_P\, \delta\mathcal{F}_\eta/\delta\Phi\big]\, \mathrm{d}t + \beta^{-1}\, \tfrac{1}{2}\, \mathrm{Tr}\big[\mathcal{M}_P^{1/2} D^2F(\Phi)\, \mathcal{M}_P^{1/2}\big]\mathrm{d}t \\ + DF(\Phi)\, \mathcal{M}_P^{1/2}\, \mathrm{d}W_t \;+\; \text{(boundary terms from (9))}. \end{aligned}$$

We apply $F = S_i$ and then the quotient rule $p_i = S_i/S_{\mathrm{tot}}$ with $S_{\mathrm{tot}} := \sum_j S_j$. The derivatives $DS_i(\Phi)$ and $D^2S_i(\Phi)$ act via the chain rule on $T\Phi$ restricted to Γ_i, yielding local multipliers proportional to $f'(s)$ and $f''(s)$.

3.2. Projected Order Parameters and Limiting SDE

The resulting evolution for $p_i(t)$ can be written as

$$\mathrm{d}p_i(t) \;=\; b_i\big(\Phi(t)\big)\, \mathrm{d}t \;+\; \sum_k \sigma_{ik}\big(\Phi(t)\big)\, \mathrm{d}W_k(t) \;+\; \sum_\ell \tilde{\sigma}_{i\ell}\big(\Phi(t)\big)\, \mathrm{d}B_\ell(t), \tag{10}$$

where W_k, B_ℓ are the coordinates of W and B in orthonormal bases, and b_i, σ_{ik}, $\tilde{\sigma}_{i\ell}$ are obtained from DS_i, D^2S_i, the mobilities, and the trace. By Assumption 13, the quadratic variation of p is governed by the reversible Dirichlet form of $\mathcal{F}_\eta$; b_i is induced by the deterministic part of (8)–(9) plus the Itô correction.

We now perform a *diffusive rescaling* that averages out fast boundary fluctuations in the alignment layer, following standard diffusion-approximation theory [31]. Fix a scale parameter $\varepsilon \downarrow 0$ and define

$$p^{(\varepsilon)}(t) := p\big(\Phi(t/\varepsilon^2)\big).$$

Under time–scale separation (fast relaxation of Φ at fixed p) and mixing in the boundary layer, weak convergence of $p^{(\varepsilon)}$ to a Markov diffusion p on Δ^{m-1} holds with generator

$$\mathcal{L}f(p) \;=\; \frac{1}{2} \sum_{i,j=1}^m a_{ij}(p)\, \partial_{ij} f(p) \;+\; \sum_{i=1}^m b_i^*(p)\, \partial_i f(p), \tag{11}$$

where the effective covariance $a(p)$ and drift $b^*(p)$ are obtained by fluctuation-averaging [73]. Permutation symmetry of channels and invariance under rigid motions preserving Φ_A imply that $a(p)$ has the *Wright–Fisher* form [31,33]

$$a_{ij}(p) \;=\; \alpha\, \big(\delta_{ij}\, p_i \;-\; p_i p_j\big), \qquad \alpha > 0, \tag{12}$$

where $\alpha = \alpha(\beta, \eta, \kappa, \lambda_{\mathrm{eff}}, \xi_b, \Gamma)$ is a scalar *boundary diffusion intensity*. Detailed balance at the interface enforces *zero effective drift* [86]:

$$b_i^*(p) \;\equiv\; 0, \qquad i = 1, \ldots, m. \tag{13}$$

 doi:10.20944/preprints202508.2056.v1

Finally, the absorbing condition at faces $\{p_i = 1\}$ follows from standard boundary classification for absorbing Wright–Fisher diffusions [33].

A canonical SDE representation of (11)–(12) is

$$\mathrm{d}p_i(t) \;=\; \sum_{j=1}^{m} \sqrt{\alpha}\,\Big(\delta_{ij} - p_j(t)\Big)\,\sqrt{p_i(t)}\,\mathrm{d}W_{ij}(t) \;-\; \sqrt{\alpha}\,p_i(t)\sum_{j=1}^{m}\sqrt{p_j(t)}\,\mathrm{d}W_{ji}(t), \tag{14}$$

where $\{W_{ij}\}_{i,j=1}^{m}$ is a matrix of independent standard Brownian motions. The form (14) is a standard Wright–Fisher diffusion representation [31,33]; it preserves the simplex constraint $\sum_i p_i \equiv 1$ and ensures $p_i \in [0,1]$ almost surely.

Assumption 16 (Regularity and symmetry)**.** We assume:

(R1) (*Local Lipschitz & non–explosion*) The coefficients in (10) are locally Lipschitz in Φ in a tubular neighbourhood of the alignment manifold and have at most linear growth; solutions remain in a compact subset of $H^1(U)$ with high probability on bounded times [17].

(R2) (*Boundary mixing & time–scale separation*) The alignment layer near Γ is rapidly mixing on time scale $o(\varepsilon^{-2})$; conditional on p, the fast variables are ergodic with a unique reversible measure induced by $\mu_{\beta,\eta}$, and their autocovariances are integrable, consistent with homogenization theory [73].

(R3) (*Channel symmetry*) The geometry and noise are invariant under permutations of $\{\Gamma_i\}$ and under isometries of Γ that preserve Φ_{A}; f is fixed once and for all.

(R4) (*Absorbing vertices*) If $p_i = 1$ for some i, then the limiting dynamics leaves p at e_i almost surely, in analogy with absorbing boundaries in Wright–Fisher diffusions [33].

Under (R1)–(R4), the diffusion limit exists, is unique in law, has generator (11) with a as in (12) and $b^* \equiv 0$, and takes values in Δ^{m-1} with absorbing vertices $\{e_i\}$ [31].

Theorem 3.1 (Diffusion limit on the outcome simplex)**.** *Let $p^{(\varepsilon)}(t) = p(\Phi(t/\varepsilon^2))$ be the rescaled overlap process associated with (8)–(9). Suppose Assumptions 13, 14, and 16 hold. Then, as $\varepsilon \downarrow 0$, the laws of $\{p^{(\varepsilon)}\}_{\varepsilon>0}$ on $D([0,T],\Delta^{m-1})$ are tight and converge weakly to the unique solution of the martingale problem for the generator $\mathcal{L}$ in (11) with covariance (12) and zero drift (13), subject to absorbing boundary condition at the vertices [31,86]. Equivalently, $p^{(\varepsilon)} \Rightarrow p$ where p solves (14) on Δ^{m-1} with absorption at $\{e_i\}$.*

Proof sketch. Tightness follows from Aldous' criterion [1] using (R1) and uniform moment bounds derived from the reversible Dirichlet form. Identification of the limit uses the martingale problem framework [31,86]: for smooth f, $f(p^{(\varepsilon)}(t)) - f(p^{(\varepsilon)}(0)) - \int_0^t \mathcal{L}^{(\varepsilon)} f(p^{(\varepsilon)}(s))\,\mathrm{d}s$ is a martingale, where $\mathcal{L}^{(\varepsilon)}$ is computed from (10). Under (R2), $\mathcal{L}^{(\varepsilon)} f \to \mathcal{L} f$ with covariance (12) obtained by Green–Kubo formulas for boundary fluctuations [42], and under detailed balance (Assumption 13) the effective drift vanishes. Absorption (R4) is inherited by the limit. Uniqueness in law for (14) with degenerate diffusion on Δ^{m-1} is standard [31,33]. □

4. Martingale Structure and Absorption Probabilities

4.1. Zero–Drift Structure from Detailed Balance

For the limiting diffusion of Theorem 3.1, detailed balance at the interface (Assumption 13), together with channel symmetry (R3), implies $b_i^* \equiv 0$ in (11). Intuitively, in the neutral (symmetric) alignment landscape the apparatus does not bias transitions between channels; the stochastic fluctuations are balanced and purely diffusive on Δ^{m-1} [31].

Proposition 17 (Martingale property)**.** *Let $p(t)$ be the Δ^{m-1}–valued diffusion of Theorem 3.1. Then for each $i = 1,\dots,m$, $p_i(t)$ is a bounded martingale with respect to the natural filtration up to the absorption time $\tau := \inf\{t \geq 0 :\; p(t) \in \{e_1,\dots,e_m\}\}$. In particular, $\mathbb{E}[p_i(t \wedge \tau)] = \mathbb{E}[p_i(0)]$ for all $t \geq 0$.*

Proof. With generator (11) and $b^* \equiv 0$, we have for the linear coordinate p_i that $\partial_{jk} p_i \equiv 0$ for all j,k and hence

$$\mathcal{L}p_i(p) \;=\; \tfrac{1}{2}\sum_{j,k} a_{jk}(p)\,\partial_{jk}p_i \;=\; 0.$$

 doi:10.20944/preprints202508.2056.v1

Thus $p_i(t) - p_i(0) - \int_0^t \mathcal{L}p_i(p(s))\,\mathrm{d}s = p_i(t) - p_i(0)$ is a local martingale [86]. Since $0 \le p_i \le 1$, it is bounded and therefore a true martingale. Stopping at $\tau \wedge t$ preserves the martingale property. □

4.2. Optional stopping and Born weights

Let e_i denote the ith vertex of Δ^{m-1} (the pure ith channel). Define τ as above.

Theorem 4.1 (Single–shot Born probabilities)**.** *Assume the hypotheses of Theorem 3.1 and Proposition 17. Then*

$$\mathbb{P}\big(p(\tau) = e_i\big) \;=\; \mathbb{E}\big[p_i(\tau)\big] \;=\; \mathbb{E}\big[p_i(0)\big] \;=\; p_i(0).$$

If the microdomain is prepared with initial overlaps $p_i(0) = |c_i|^2$ relative to the apparatus eigen–domains, the absorption probabilities equal the Born weights $|c_i|^2$.

Proof sketch. By Proposition 17, $p_i(t \wedge \tau)$ is a bounded martingale, hence uniformly integrable; Doob's optional stopping theorem [26,28] gives $\mathbb{E}[p_i(\tau)] = \mathbb{E}[p_i(0)]$. Since $p(\tau) \in \{e_1, \ldots, e_m\}$, $p_i(\tau) = \mathbf{1}_{\{p(\tau)=e_i\}}$, so $\mathbb{E}[p_i(\tau)] = \mathbb{P}(p(\tau) = e_i)$. □

See Appendix N for the full proof.

4.3. Hitting, Non-Explosion, and Boundary Behavior

Lemma 18 (Almost sure absorption and integrability of τ)**.** *For the Wright–Fisher diffusion (14) (equivalently, generator (11) with (12)) on Δ^{m-1} with zero drift and no mutation, the process is absorbed at a vertex in finite time almost surely: $\mathbb{P}(\tau < \infty) = 1$. Moreover, $\mathbb{E}[\tau] < \infty$.*

Proof sketch. In the neutral Wright–Fisher diffusion with m types and no mutation, standard boundary classification shows that the boundary $\partial\Delta^{m-1}$ is attainable and absorbing [31,33]. Successive extinction of types occurs until fixation at a vertex. Lyapunov functions of the form $V(p) = \sum_i p_i(1 - p_i)$ satisfy $\mathcal{L}V \le -c \sum_{i<j} p_i p_j$ away from vertices, implying that V is a strict supermartingale and giving finiteness of $\mathbb{E}[\tau]$ by Foster–Lyapunov criteria [66]. See Appendix M for details. □

Consequence.

Lemmas 18 and Proposition 17 justify optional stopping in Theorem 4.1 and complete the single–shot Born–rule derivation under the chronon alignment dynamics. See Appendix N for the full proof.

5. Collapse, Definiteness, and the Outcome Simplex

In standard quantum mechanics, the measurement problem centers on how a quantum system, initially described by a coherent superposition, yields a single, definite outcome upon observation. The traditional response is the *wavefunction collapse postulate*, an explicit discontinuous update to the system's state conditioned on measurement [90]. This section interprets how Chronon Field Theory (ChFT) resolves this issue dynamically, by replacing postulated collapse with stochastic absorption in the outcome simplex.

5.1. Collapse as Stochastic Absorption

Let $p(t) \in \Delta_{m-1}$ denote the time-dependent overlap vector encoding the alignment of the chronon field with the m apparatus eigen–domains (Definition 7). As shown in Proposition 17, each coordinate $p_i(t)$ is a bounded martingale under the interface-coupled chronon dynamics, and the process is absorbed almost surely at one of the simplex vertices $\{e_i\}$ in finite time τ (Lemma 18).

This absorption event corresponds to a physical measurement outcome. Specifically, absorption at e_i implies that channel i dominates the alignment, i.e.,

$$p(\tau) = e_i \quad \Rightarrow \quad p_j(\tau) = \delta_{ij} \quad \text{for all } j.$$

 doi:10.20944/preprints202508.2056.v1

The field configuration Φ^μ becomes fully aligned with the ith apparatus eigen–domain, and this alignment is macroscopically stable due to the properties of the stabilized apparatus region $\mathcal{A}$ (Definition 1). Thus, the measurement produces a definite, classically recordable outcome without the need to invoke discontinuous projection or nonlocal effects.

5.2. Comparison to Conventional Collapse

This absorption-based mechanism fulfills the empirical role of wavefunction collapse but arises here as an emergent property of local, reversible, and stochastic dynamics at the boundary layer:

- The outcome is *definite* due to absorption: the system eventually enters a simplex vertex state e_i, excluding all other outcomes.
- The process is *probabilistic* via martingale properties: the absorption probabilities are given by the initial overlaps $p_i(0)$, reproducing the Born rule (Theorem 4.1).
- The dynamics is *local and continuous* in spacetime: all stochasticity originates from chronon fluctuations at the measurement interface Γ, governed by reversible SPDEs (Section 3).

In contrast to standard collapse models (e.g., GRW [39]), no additional dynamics or modification of Schrödinger evolution is introduced. Unlike purely epistemic views [46,84], the stochasticity arises from an objectively fluctuating alignment process. Compared to quantum trajectory or stochastic Schrödinger frameworks [5,22,40], the present derivation ties the martingale and absorption structure to coarse–grained, classical field interactions, rather than postulating stochasticity at the level of the wavefunction.

5.3. System Eigenstates versus Apparatus Eigen–Domains

In the textbook formulation of quantum measurement, a system initially prepared in a superposition

$$|\psi\rangle = \sum_i c_i |\psi_i\rangle$$

of eigenstates $\{|\psi_i\rangle\}$ of some observable O is said to "collapse" into one of these eigenstates upon measurement, with Born probability $|c_i|^2$. The apparatus is then taken to record this outcome by correlating its pointer state $|A_i\rangle$ with the corresponding eigenstate of the system.

Chronon Field Theory (ChFT) reformulates this picture. In CFT, the apparatus is not a passive recorder but an active dynamical system that defines a finite set of stable, coarse–grained alignment channels, or *eigen–domains*. The chronon field of the microscopic system couples to these domains across the measurement interface Γ, and its effective alignment process is described by the overlap vector $p(t)$. As shown in Section 5, the overlaps undergo a martingale diffusion and are absorbed almost surely at a simplex vertex e_i, corresponding to one of the apparatus eigen–domains. In this sense, the measurement outcome is realized as *absorption of the system's chronon field into a pre–existing apparatus channel*, rather than collapse of the system into its own eigenstate.

The two perspectives are consistent once the apparatus is designed so that its eigen–domains are *engineered to correspond to the eigenbasis of the measured observable*. For example, in a Stern–Gerlach experiment the apparatus field geometry implements two stable alignment domains corresponding to "spin up" and "spin down" along the chosen axis. What the textbook account describes as collapse of the spin state into $|\uparrow\rangle$ or $|\downarrow\rangle$ is, in CFT, realized dynamically as absorption of the chronon alignment into one of the two apparatus domains. The Born probabilities arise from the initial overlaps $p_i(0) = |c_i|^2$ and the martingale absorption law.

This reframing highlights a key conceptual advance: in CFT the *apparatus, not the system, determines the measurement basis*. The eigen–domains are stabilized features of the macroscopic apparatus field, and the system's stochastic alignment with them yields both definiteness and Born weights. Thus, CFT explains dynamically why a particular set of outcomes is available at all, while reproducing the standard quantum prediction that the system is "found in an eigenstate" of the chosen observable.

See Figure 2 for a visual illustration.

 doi:10.20944/preprints202508.2056.v1

(a) Apparatus eigen–domains and boundary alignment

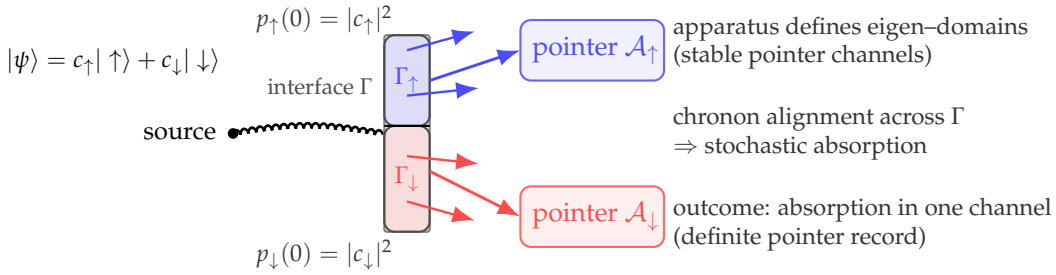

(b) Outcome simplex and absorption (Born weights)

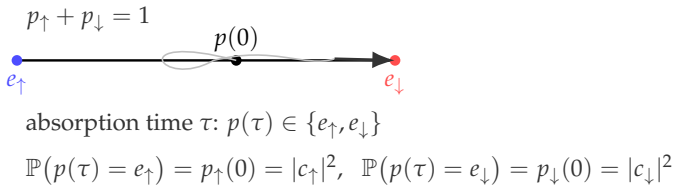

Figure 2. (a) The apparatus defines stabilized eigen–domains $\Gamma_\uparrow, \Gamma_\downarrow$ on the interface Γ. A microscopic chronon field, prepared in a superposition $|\psi\rangle = c_\uparrow|\uparrow\rangle + c_\downarrow|\downarrow\rangle$, couples locally to Γ and stochastically *aligns* with one domain. (b) The overlap process $p(t) \in \Delta_1$ diffuses as a bounded martingale and is absorbed at a vertex e_i; the hitting probabilities equal the initial overlaps (Born rule).

5.4. Definiteness without Projection

The key insight is that outcome definiteness is dynamically encoded in the *absorbing boundary structure* of the outcome simplex Δ_{m-1}. Once the process reaches a vertex e_i, it remains there with probability one, reflecting irreversible alignment with a single apparatus domain. This yields a natural resolution of the measurement problem within CFT:

$$\text{Initial superposition} \longrightarrow \text{Stochastic alignment} \longrightarrow \text{Absorbing outcome.}$$

Collapse is thus reinterpreted as an emergent, irreversible flow toward absorbing states in the geometry of alignment overlaps, replacing the postulated discontinuity of traditional interpretations.

5.5. Interpretational Implications

This reinterpretation of collapse as absorption supports several key principles:

1. *Locality*: All causal influences are confined to the measurement interface and its neighborhood.
2. *No superluminal effects*: Alignment propagation respects the apparatus foliation and causal structure induced by $\Phi^{\mu}_{\mathcal{A}}$.
3. *Objective definiteness*: The selection of an outcome is a physical stochastic process with classical records encoded in macroscopic apparatus channels.
4. *No auxiliary postulates*: The Born rule and outcome definiteness follow directly from the chronon field dynamics and interface coupling.

In this way, CFT offers a conceptually and mathematically coherent resolution of the collapse problem by grounding it in physically well-defined stochastic geometry.

 doi:10.20944/preprints202508.2056.v1

6. Hydrodynamic Limit from Chronon Microdynamics

6.1. Microscopic Model, Scaling, and Tightness

We resolve the diffusion limit of Section 3 directly from the microscopic chronon dynamics in a boundary layer around the interface Γ. Let $\ell_{\mathrm{uv}} > 0$ be the microscopic spacing and let $\xi \gg \ell_{\mathrm{uv}}$ be the coarse–graining scale. For a small parameter $\varepsilon \downarrow 0$ we consider a family of discretizations with

$$\ell_{\mathrm{uv}} = \ell_{\mathrm{uv}}(\varepsilon) \to 0, \qquad \xi = \xi(\varepsilon) \to 0, \qquad \xi/\ell_{\mathrm{uv}} \to \infty,$$

and a fixed physical interface $\Gamma \subset \Sigma_{\tau_0}$ covered by a *boundary layer* $U_\Gamma^{(\varepsilon)} := \{x : \mathrm{dist}(x,\Gamma) \le c\,\xi(\varepsilon)\}$.

Let $\Lambda^{(\varepsilon)} \subset U_\Gamma^{(\varepsilon)}$ be the set of lattice sites, and let $\Gamma^{(\varepsilon)} \subset \Lambda^{(\varepsilon)}$ denote boundary sites (one layer thick) identified with Γ via nearest–point projection. Channels are discrete partitions $\Gamma^{(\varepsilon)} = \bigsqcup_{i=1}^m \Gamma_i^{(\varepsilon)}$ refining the continuum $\{\Gamma_i\}_{i=1}^m$.

Microscopic stochastic dynamics.

At each $r \in \Lambda^{(\varepsilon)}$ we have a microscopic chronon vector $X_r \in \mathbb{R}^{1,d}$. The stochastic dynamics is the overdamped Langevin system consistent with the discrete version of the alignment functional (7), in the spirit of interacting particle systems with Gibbs stationary measures [85]:

$$\mathrm{d}X_r(t) = -\,\partial_{X_r} H_\eta^{(\varepsilon)}(X(t))\,\mathrm{d}t \;+\; \sqrt{2\beta^{-1}}\,\mathrm{d}W_r(t), \qquad r \in \Lambda^{(\varepsilon)} \setminus \Gamma^{(\varepsilon)}, \tag{15}$$

$$\mathrm{d}X_r(t) = -\,\partial_{X_r} H_\eta^{(\varepsilon)}(X(t))\,\mathrm{d}t \;+\; \sqrt{2\beta^{-1}}\,\mathrm{d}B_r(t), \qquad r \in \Gamma^{(\varepsilon)}, \tag{16}$$

where $H_\eta^{(\varepsilon)}$ is the discrete energy plus a boundary penalty

$$H_\eta^{(\varepsilon)}(X) \;=\; -\frac{1}{2} \sum_{\substack{r,q \in \Lambda^{(\varepsilon)} \\ \mathrm{dist}(r,q) \le R_{\mathrm{int}}}} J_{rq}\, X_r \cdot X_q \;+\; \sum_{r \in \Lambda^{(\varepsilon)}} V(X_r \cdot X_r) \;+\; \eta \sum_{r \in \Gamma^{(\varepsilon)}} \big(1 - \Phi_{\mathrm{A}}(r) \cdot X_r\big)^2.$$

Here W_r, B_r are independent standard Brownian motions in $\mathbb{R}^{1,d}$, and $\cdot$ is the Minkowski inner product. The unique invariant measure is the discrete Gibbs measure $\propto \exp(-\beta H_\eta^{(\varepsilon)}(X))$ by detailed balance [55].

Block averages and overlap observables.

On mesoscopic blocks $B_a^{(\varepsilon)}$ (diameter ξ) define $\Phi_a := |B_a^{(\varepsilon)}|^{-1} \sum_{r \in B_a^{(\varepsilon)}} X_r$, and interpolate to a field $\Phi^{(\varepsilon)}$. The discrete alignment scalar on a boundary site $r \in \Gamma^{(\varepsilon)}$ is

$$s_r := -\,\Phi_{\mathrm{A}}(r) \cdot X_r \quad (\ge 1 \text{ near alignment}),$$

and the discrete channel strengths and overlaps are

$$S_i^{(\varepsilon)}(t) := \sum_{r \in \Gamma_i^{(\varepsilon)}} \omega_r^{(\varepsilon)}\, f\big(s_r(t)\big), \qquad p_i^{(\varepsilon)}(t) := \frac{S_i^{(\varepsilon)}(t)}{\sum_{j=1}^m S_j^{(\varepsilon)}(t)}, \tag{17}$$

with weights $\omega_r^{(\varepsilon)}$ approximating the surface element on Γ. By Lemma 8 (trace continuity), $p^{(\varepsilon)}(t)$ approximates the continuum $p(t)$ as $\varepsilon \to 0$.

Semimartingale decomposition.

Applying Itô to (17) and using (15)–(16), each $S_i^{(\varepsilon)}$ admits the decomposition

$$S_i^{(\varepsilon)}(t) \;=\; S_i^{(\varepsilon)}(0) \;+\; \int_0^t I_i^{(\varepsilon)}(s)\,\mathrm{d}s \;+\; M_i^{(\varepsilon)}(t), \tag{18}$$

 doi:10.20944/preprints202508.2056.v1

where $M_i^{(\varepsilon)}$ is a martingale and $I_i^{(\varepsilon)}$ is the compensator (drift). Quadratic covariations satisfy

$$[M_i^{(\varepsilon)}, M_j^{(\varepsilon)}]_t \;=\; \int_0^t C_{ij}^{(\varepsilon)}(s)\,\mathrm{d}s, \qquad C_{ij}^{(\varepsilon)}(s) \;=\; 2\beta^{-1}\sum_{r\in\Gamma^{(\varepsilon)}} \omega_r^{(\varepsilon)2}\,\partial_{X_r}S_i^{(\varepsilon)}\,\partial_{X_r}S_j^{(\varepsilon)}\big|_{X(s)}. \tag{19}$$

A ratio Itô calculation yields a semimartingale form for $p_i^{(\varepsilon)}$ with drift $b_i^{(\varepsilon)}$ and covariance $a_{ij}^{(\varepsilon)}$ built from $I^{(\varepsilon)}$ and $C^{(\varepsilon)}$ [55,88].

Assumption 19 (Mixing and propagation of chaos)**.** There exist constants $c_0, \lambda_{\mathrm{mix}}, \tau_{\mathrm{mix}} > 0$ independent of ε such that:

(C1) (*Uniform spectral gap / mixing*) The generator of (15)–(16) restricted to $U_\Gamma^{(\varepsilon)}$ has spectral gap $\geq \lambda_{\mathrm{mix}}$, and time autocorrelations of local observables $F(X_t)$ supported in balls of radius ξ decay as $\exp(-t/\tau_{\mathrm{mix}})$, as ensured by Poincaré/log–Sobolev inequalities for reversible lattice systems [2,49,96].

(C2) (*Propagation of chaos across channels*) For disjoint channel subsets $A, B \subset \Gamma^{(\varepsilon)}$ separated by $\mathrm{dist}(A,B) \geq c_0\,\xi$, the covariance of bounded Lipschitz observables $F(X|_A)$ and $G(X|_B)$ under the invariant measure is $\mathcal{O}(\exp(-\mathrm{dist}(A,B)/\xi))$, consistent with exponential decay of correlations in the Dobrushin uniqueness/cluster–expansion regime [23,24,85].

(C3) (*Boundary fast scale*) The relaxation/mixing times satisfy $\tau_{\mathrm{mix}} = o(\varepsilon^{-2})$ under the diffusive rescaling $t \mapsto t/\varepsilon^2$ used below, as in standard hydrodynamic scaling for reversible particle systems [55].

Theorem 6.1 (Tightness and identification of the limit)**.** *Let $p^{(\varepsilon)}(t) := p^{(\varepsilon)}(t/\varepsilon^2)$ be the diffusively rescaled overlap process constructed from (17). Assume regularity (Assumption 16), detailed balance at the boundary (Appendix P), well–posedness of the projected SDE (Appendix M), and mixing/chaos (Assumption 19). Then:*

(i) (Tightness) *The family $\{p^{(\varepsilon)}\}_{\varepsilon>0}$ is tight in $D([0,T],\Delta^{m-1})$ for each $T<\infty$ by the Aldous–Rebolledo criterion for semimartingales [1,79,80].*

(ii) (Limit generator) *Any weak limit p solves the martingale problem on Δ^{m-1} with generator*

$$\mathcal{L}f(p) \;=\; \frac{1}{2}\sum_{i,j=1}^{m} a_{ij}(p)\,\partial_{ij}f(p) \;+\; \sum_{i=1}^{m} b_i^*(p)\,\partial_i f(p),$$

where the coefficients arise from fluctuation averaging/Green–Kubo formulas for reversible dynamics [31,42,56,73]:

$$a_{ij}(p) = \lim_{\varepsilon\downarrow 0}\,\mathbb{E}_{\mu_{\beta,\eta}}\Big[\int_0^\infty \mathbb{E}\Big(\dot p_i^{(\varepsilon)}(0)\,\dot p_j^{(\varepsilon)}(t)\;\big|\;p^{(\varepsilon)}(0)=p\Big)\,\mathrm{d}t\Big], \tag{20}$$

$$b_i^*(p) = \lim_{\varepsilon\downarrow 0}\,\mathbb{E}_{\mu_{\beta,\eta}}\Big[b_i^{(\varepsilon)}(0)\;\big|\;p^{(\varepsilon)}(0)=p\Big]. \tag{21}$$

(iii) (Wright–Fisher form and zero drift) *By channel symmetry and reversibility, $a_{ij}(p) = \alpha\,(\delta_{ij}p_i - p_ip_j)$ and $b_i^*(p)\equiv 0$ [31,33,86].*

Consequently, p is the Wright–Fisher diffusion on Δ^{m-1} with absorbing vertices as in Theorem 3.1.

Proof sketch. *(i) Tightness:* The semimartingale decomposition (18) and the ratio Itô formula give

$$p_i^{(\varepsilon)}(t) = p_i^{(\varepsilon)}(0) + \int_0^t b_i^{(\varepsilon)}(s)\,\mathrm{d}s + M_i^{(\varepsilon)}(t),$$

 doi:10.20944/preprints202508.2056.v1

with predictable quadratic variation $[M_i^{(\varepsilon)}]_t = \int_0^t a_{ii}^{(\varepsilon)}(s)\,\mathrm{d}s$. Under (C1)–(C3), $b^{(\varepsilon)}$ and $a^{(\varepsilon)}$ are uniformly controlled, so Aldous–Rebolledo tightness applies [1,79,80].
(ii) Identification uses the martingale–problem method [31]: for smooth f,

$$f(p^{(\varepsilon)}(t)) - f(p^{(\varepsilon)}(0)) - \int_0^t \mathcal{L}^{(\varepsilon)} f(p^{(\varepsilon)}(s))\,\mathrm{d}s$$

is a martingale, where $\mathcal{L}^{(\varepsilon)}$ is computed from $b^{(\varepsilon)}, a^{(\varepsilon)}$; mixing yields $\mathcal{L}^{(\varepsilon)} \to \mathcal{L}$ in the Green–Kubo sense [42,56,73].
(iii) Symmetry forces isotropy on the tangent space $\{\sum_i u_i = 0\}$, giving the Wright–Fisher covariance; reversibility (detailed balance) kills the averaged drift [86]. Absorption follows because once a channel monopolizes the boundary weight, cross–channel fluctuation terms vanish. □

6.2. Boundary Layer and Coefficient Identification

We now express the limiting covariance intensity α in terms of boundary fluctuations (FDT) and quantify drift cancellation and error rates.

Alignment currents and Green–Kubo formula.

Let $\dot{S}_i^{(\varepsilon)}(t)$ denote the stochastic time derivative of $S_i^{(\varepsilon)}(t)$ in (17). Define the (centered) *alignment currents*

$$J_i^{(\varepsilon)}(t) \;:=\; \dot{S}_i^{(\varepsilon)}(t) \;-\; \mathbb{E}_{\mu_{\beta,\eta}}\big[\dot{S}_i^{(\varepsilon)} \,\big|\, p^{(\varepsilon)}(t)\big],$$

which are square–integrable martingale noises supported in the boundary layer. Then, under Assumption 19, a Green–Kubo representation of α is [42,56,85]

$$\alpha \;=\; \lim_{\varepsilon\downarrow 0} \frac{1}{\big(S_{\mathrm{tot}}^{(\varepsilon)}\big)^2} \sum_{i=1}^{m}\sum_{j=1}^{m} \int_0^\infty \mathbb{E}_{\mu_{\beta,\eta}}\Big[J_i^{(\varepsilon)}(0)\, J_j^{(\varepsilon)}(t) \,\Big|\, p^{(\varepsilon)}(0) = p\Big]\,\mathrm{d}t, \tag{22}$$

where $S_{\mathrm{tot}}^{(\varepsilon)} = \sum_k S_k^{(\varepsilon)}$. Channel symmetry reduces (22) to a single scalar $\alpha = \alpha(\beta, \eta, \kappa, \lambda_{\mathrm{eff}}, \xi, \Gamma)$.

Drift cancellation by detailed balance.

The raw drift $b_i^{(\varepsilon)}$ is the conditional expectation of $\dot{p}_i^{(\varepsilon)}$ given $p^{(\varepsilon)}$. Detailed balance and invariance under channel permutations imply

$$\mathbb{E}_{\mu_{\beta,\eta}}\Big[\dot{p}_i^{(\varepsilon)}(t) \,\Big|\, p^{(\varepsilon)}(t) = p\Big] \;\equiv\; 0,$$

so $b_i^*(p) = 0$ in the limit [55,86]. If small asymmetries (e.g. Γ_i areas not exactly equal or weak channel–dependent mobilities) are present, then

$$\sup_{p\in\Delta^{m-1}} |b_i^*(p)| \;\le\; C\Big(\|\mathrm{asym}\| \;+\; \eta^{-1/2} \;+\; \beta^{-1/2}\Big), \tag{23}$$

for a constant C depending on geometry and regularity; thus the Born probabilities are stable to first order.

Rates and boundary thickness.

Let λ_{mix} be the spectral gap from (C1) and let τ_{mix} be the mixing time. Then for $t \le T$ and small ε,

$$\sup_{f\in C_b^2(\Delta^{m-1})} \Big|\mathbb{E}\big[f(p^{(\varepsilon)}(t))\big] - \mathbb{E}\big[f(p(t))\big]\Big| \;\le\; C_T\left(\frac{1}{\sqrt{\lambda_{\mathrm{mix}}\,\xi/\ell_{\mathrm{uv}}}} \;+\; \frac{\tau_{\mathrm{mix}}}{\varepsilon^{-2}}\right),$$

so convergence in law holds with an explicit qualitative rate provided λ_{mix} is bounded away from zero and $\tau_{\mathrm{mix}} = o(\varepsilon^{-2})$, reflecting spectral–gap/log–Sobolev control of relaxation [2,62]. The coefficient

 doi:10.20944/preprints202508.2056.v1

α scales linearly with the effective boundary mobility and inversely with the channel areas in the symmetric case,

$$\alpha \asymp \frac{\beta^{-1}\,\mathrm{Mob}_\Gamma}{\mathrm{Area}_\gamma(\Gamma)} \quad \text{(symmetric channels, } f(r)=r^2\text{)},$$

up to dimensionless factors depending smoothly on $(\kappa, \lambda_{\mathrm{eff}})$, in line with Green–Kubo/hydrodynamic scaling [85].

Remark 20 (Absorbing faces in the microscopic model). In the discrete dynamics, once $S_i^{(\varepsilon)} = S_{\mathrm{tot}}^{(\varepsilon)}$ (all boundary spins aligned to channel i so $p_i^{(\varepsilon)} = 1$) the coupling terms between distinct channels vanish and only intra–channel fluctuations remain, which preserve $p_i^{(\varepsilon)} = 1$. This yields the absorbing vertices in the limit.

Remark 21 (Choice of f and universality of the limit). The choice of the increasing function f in (17) affects microscopic weights $S_i^{(\varepsilon)}$ but not the limiting *normalized* process p: after normalization, the diffusion matrix must be tangent to the simplex and isotropic under channel permutations, forcing the Wright–Fisher form [31,33]. Hence the limiting law of p is universal within the class of smooth strictly increasing f.

7. Large Deviations for Empirical Frequencies

7.1. IID Repetition from Absorption Law

Fix an apparatus with channels $\{\Gamma_i\}_{i=1}^m$ and initial overlap vector $p^\star = (p_1^\star, \dots, p_m^\star) \in \Delta^{m-1}$ for the prepared microdomain on the interface leaf Σ_{τ_0}. Let $p(t)$ be the Wright–Fisher diffusion on Δ^{m-1} of Theorem 3.1 with zero drift and absorbing vertices $\{e_i\}$, started at $p(0) = p^\star$. Let $\tau := \inf\{t \geq 0 : p(t) \in \{e_1, \dots, e_m\}\}$ be the absorption time (finite a.s., Lemma 18), and define the outcome random variable

$$Y := i \quad \Longleftrightarrow \quad p(\tau) = e_i \quad (i = 1, \dots, m).$$

By Theorem 4.1, $\mathbb{P}(Y = i) = p_i^\star$ (Born weights).

A *trial* is one prepare–evolve–absorb cycle followed by a reset of the apparatus boundary layer to its stationary macrostate and a fresh preparation with the same overlap $p^\star$. Let $(Y_k)_{k\geq 1}$ be the outcomes from such trials, and let $N \in \mathbb{N}$ be the number of repetitions.

Independence/mixing assumptions. We work under either:

(A1) **IID trials.** The apparatus reset fully decorrelates successive trials and the prepared microdomains are independent. Thus (Y_k) are i.i.d. with common law $p^\star$ on $\{1, \dots, m\}$.

(A2) **Fast mixing trials.** (Y_k) is strictly stationary and α–mixing with coefficients $(\alpha(n))_{n\geq 1}$ satisfying

$$\sum_{n\geq 1} \alpha(n)^{\delta/(2+\delta)} < \infty \quad \text{for some } \delta > 0,$$

(e.g. summable $\alpha(n)$). The one–trial marginal is still $p^\star$, ensuring applicability of mixing LDPs [10,18].

Define the empirical frequency vector $\hat{f}_N \in \Delta^{m-1}$ by

$$\hat{f}_N(i) := \frac{1}{N}\sum_{k=1}^N \mathbf{1}_{\{Y_k = i\}}, \qquad i = 1, \dots, m.$$

Theorem 7.1 (Sanov LDP for outcome frequencies)**.** *Let (Y_k) be generated by the absorption law with single–trial distribution $p^\star \in \Delta^{m-1}$. Then $(\hat{f}_N)$ satisfies a large–deviation principle on Δ^{m-1} with speed N and good, convex rate function*

$$I(q) = D(q \,\|\, p^\star) = \sum_{i=1}^m q_i \log \frac{q_i}{p_i^\star},$$

 doi:10.20944/preprints202508.2056.v1

with the conventions $0\log(0/p) = 0$ *and* $I(q) = +\infty$ *if* $q_i > 0$ *for some* i *with* $p_i^\star = 0$. *This holds under either:*

(i) IID case (A1): *classical Sanov theorem [19,82];* $I(q) \geq 0$ *and* $I(q) = 0$ *iff* $q = p^\star$.

(ii) Mixing case (A2): *Sanov–type LDP with the same speed and rate* I *by LDP results for mixing sequences [10,18].*

Consequently, for any closed $F \subset \Delta^{m-1}$ *and open* $G \subset \Delta^{m-1}$,

$$\limsup_{N\to\infty} \frac{1}{N} \log \mathbb{P}(\hat{f}_N \in F) \leq -\inf_{q\in F} I(q), \qquad \liminf_{N\to\infty} \frac{1}{N} \log \mathbb{P}(\hat{f}_N \in G) \geq -\inf_{q\in G} I(q),$$

and $\hat{f}_N \to p^\star$ *almost surely, with exponentially small tail probabilities governed by* I.

Proof sketch. (i) Under (A1), (Y_k) are i.i.d. with law $p^\star$, so Sanov's theorem applies; on a finite alphabet the rate is $D(q\|p^\star)$.

(ii) Under (A2), level–2 LDPs for strictly stationary α–mixing sequences with sufficiently decaying mixing coefficients hold with the same Cramér transform as in the i.i.d. case [10]. Since the single–trial SCGF remains $\Lambda(\theta) = \log \sum_i p_i^\star e^{\theta_i}$ and block decoupling yields asymptotic additivity, Gärtner–Ellis [19,29] gives $I(q) = \sup_\theta\{\langle\theta, q\rangle - \Lambda(\theta)\} = D(q\|p^\star)$. □

Remarks.

(1) A CLT holds: $\sqrt{N}(\hat{f}_N - p^\star) \Rightarrow \mathcal{N}(0, \Sigma)$ with $\Sigma = \mathrm{diag}(p^\star) - p^\star(p^\star)^\top$ under (A1) [7], and with a long–range covariance correction under (A2) [18]. (2) In the i.i.d. case, Chernoff–Hoeffding bounds [48] follow from the LDP upper bound.

7.2. Alternative Thermodynamic LDP (Optional)

We sketch a thermodynamic derivation of the same rate function I via constrained free energies, avoiding explicit trial–wise independence. Consider N repetitions realized as N disjoint boundary windows $\{\Gamma^{(k)}\}_{k=1}^N$ (in time or space), each coupled to the same stabilized apparatus A and prepared with the same $p^\star$. Let $Z^{(k)}$ be the (finite–volume) boundary partition function for window k with alignment functional $\mathcal{F}_\eta$ at inverse temperature β. Write $Z_N(\theta)$ for the *tilted* partition function that weights each realization by $\exp(\sum_{k=1}^N \theta_{Y_k}) = \exp(N\langle\theta, \hat{f}_N\rangle)$.

Assumption 22 (Approximate factorization and exponential tightness)**.** There exists $\varepsilon_N \to 0$ such that, uniformly for θ on compacts,

(F1) (*Free energy additivity*) $\frac{1}{N}\log Z_N(\theta) = \Lambda(\theta) + o(1)$ with $\Lambda(\theta) = \log\big(\sum_{i=1}^m p_i^\star e^{\theta_i}\big)$.

(F2) (*Exponential tightness*) The family $\{\hat{f}_N\}$ is exponentially tight under the θ–tilted Gibbs law.

These hold, e.g., if windows are separated by buffers $\gg \xi$ so inter-window correlations are exponentially small, and if the one–window outcome law is $p^\star$ by the single–trial martingale/absorption result.

Proposition 23 (Constrained free energy and rate function)**.** *Under Assumption 22, the sequence* $(\hat{f}_N)$ *satisfies an LDP on* Δ^{m-1} *with good rate*

$$I(q) = \sup_{\theta\in\mathbb{R}^m} \{\langle\theta, q\rangle - \Lambda(\theta)\} = D(q \,\|\, p^\star).$$

Proof sketch. By Varadhan's lemma [87] (or Gärtner–Ellis [29]), the limiting SCGF is $\Lambda(\theta)$. Its Legendre–Fenchel transform is I, which equals $D(q\|p^\star)$ on Δ^{m-1}. Exponential tightness ensures a full LDP. □

Discussion.

The thermodynamic route shows that, beyond explicit i.i.d. repetitions, the large–deviation structure is controlled by the *tilted* boundary free energy, which is fixed by the single–trial law $p^\star$

 doi:10.20944/preprints202508.2056.v1

and approximate additivity. Both the stochastic (Sanov) and thermodynamic (Varadhan) derivations identify the same rate function minimized uniquely at the Born vector $p^\star$.

8. Robustness and Extensions

8.1. Imperfect Interfaces, Finite Temperature, and Small drifts

In realistic devices the interface coupling is finite ($\eta < \infty$), the boundary layer has nonzero temperature ($\beta^{-1} > 0$), and small asymmetries in channel geometry or mobility may be present. These effects can produce a small effective drift $b^*(p)$ in the limiting simplex dynamics (Section 3), in addition to (i) a bias in the initial overlaps $p(0)$ due to imperfect preparation and (ii) small deviations of the diffusion matrix from the symmetric Wright–Fisher form $a(p) = \alpha\big(\mathrm{diag}(p) - pp^\top\big)$ [31,33]. We quantify the impact on absorption probabilities.

Notation.

Let $\mathcal{L}_0 f := \frac{1}{2}\sum_{i,j} a_{ij}(p)\,\partial_{ij} f$ be the zero–drift Wright–Fisher generator with intensity $\alpha > 0$ (Theorem 3.1). Let $\mathcal{L} f := \mathcal{L}_0 f + \sum_i b_i^*(p)\,\partial_i f$ be the perturbed generator. For each vertex e_i, denote by u_i the absorption probability for $\mathcal{L}$, i.e.

$$\begin{cases} \mathcal{L} u_i = 0 & \text{in } \mathrm{ri}(\Delta^{m-1}), \\ u_i(e_j) = \delta_{ij} & \text{on vertices}, \end{cases} \tag{24}$$

interpreted in the weak sense appropriate for degenerate operators at the boundary [30,31]. For the unperturbed process, $u_i^{(0)}(p) = p_i$.

Define small parameters

$$\delta_b := \sup_{p\in\Delta^{m-1}} \frac{\|b^*(p)\|_1}{\alpha}, \qquad \delta_\eta := \eta^{-1/2}, \qquad \delta_\beta := \beta^{-1/2}, \qquad \delta_{\mathrm{geom}} := \max_i \left| \frac{\mathrm{Area}_\gamma(\Gamma_i)}{\mathrm{Area}_\gamma(\Gamma)} - \frac{1}{m} \right|.$$

Here δ_b measures drift strength relative to diffusion; δ_η and δ_β control norm pinning and thermal roughness at the boundary; δ_{geom} captures channel area asymmetry (for $f(r) = r^2$; any fixed strictly increasing f gives an equivalent measure).

Theorem 8.1 (Quantitative stability of Born weights)**.** *Assume the hypotheses of Theorem 3.1 and the hydrodynamic limit (Theorem 6.1) with small symmetry breaking so that b^* is continuous and $\|b^*\|_\infty/\alpha \ll 1$, and the diffusion matrix satisfies*

$$\big\|a(p) - \alpha(\mathrm{diag}(p) - pp^\top)\big\| \;\le\; C_a\big(\delta_\eta + \delta_\beta + \delta_{\mathrm{geom}}\big) \quad \textit{uniformly in } p \in \Delta^{m-1}.$$

Then there exists $C = C(m)$ such that, for every initial overlap $p(0) = p^\star$,

$$\Big|\, \mathbb{P}^{\mathcal{L}}\big(p(\tau) = e_i \mid p(0) = p^\star\big) \;-\; p_i^\star \,\Big| \;\le\; C\big(\delta_b \;+\; C_a(\delta_\eta + \delta_\beta + \delta_{\mathrm{geom}}) \;+\; \|p^\star - \tilde{p}^\star\|_1\big), \tag{25}$$

where $\tilde{p}^\star$ are the ideal overlaps computed with perfect pinning and symmetric channels. In particular, when $p_i^\star = |c_i|^2$ (ideal preparation), the absorption probabilities deviate from Born weights by at most the right–hand side of (25).

Proof sketch. Let u_i and $u_i^{(0)}(p) = p_i$ solve the Dirichlet problems for $\mathcal{L}$ and $\mathcal{L}_0$, respectively. A variation–of–parameters identity gives

$$\mathcal{L}_0\big(u_i - u_i^{(0)}\big) = -\,b^*\cdot\nabla u_i \;-\; \tfrac{1}{2}\mathrm{tr}\big((a - \alpha(\mathrm{diag}(p) - pp^\top))\,\nabla^2 u_i\big),$$

 doi:10.20944/preprints202508.2056.v1

with homogeneous boundary data. Weighted Schauder estimates for degenerate Wright–Fisher operators [30,31] yield

$$\|u_i - u_i^{(0)}\|_{L^\infty(\Delta^{m-1})} \;\le\; C\left(\frac{\|b^*\|_\infty}{\alpha} + \frac{\|a - \alpha(\mathrm{diag}(p) - pp^\top)\|_\infty}{\alpha}\right),$$

where $C = C(m)$ depends only on m and boundary weights. This bounds the first two terms in (25). The preparation error $\|p^\star - \tilde{p}^\star\|_1$ accounts for imperfect initial overlaps due to finite η, β and geometric asymmetries; under the regularity assumptions in Section 2, this error is $O(\delta_\eta + \delta_\beta + \delta_{\mathrm{geom}})$. Combining gives (25). □

Remark 24 (Coupling viewpoint). An alternative proof couples the perturbed diffusion with drift b^* to the neutral Wright–Fisher process by Girsanov's theorem [53,64]. A Novikov condition holds for small $\|b^*\|_\infty/\alpha$, and the total variation distance of path measures up to τ is $O(\delta_b)$, implying the same $O(\delta_b)$ bound on absorption probabilities.

8.2. Degeneracies, Continuous Spectra, and POVMs

Degenerate outcomes.

Suppose the apparatus eigen–domains are grouped into $K < m$ *degenerate bins* $\mathcal{I}_1, \dots, \mathcal{I}_K$ (e.g. identical eigenvalues or coarse readout), and only the bin label is recorded. Let $\Pi_k := \sum_{i \in \mathcal{I}_k} e_i$ be the face corresponding to bin k and define $P_k(t) := \sum_{i \in \mathcal{I}_k} p_i(t)$. By linearity of the Wright–Fisher SDE on coordinates (Appendix M), $P_k(t)$ is again a Wright–Fisher coordinate (summing components preserves martingales and absorption) [31,33]. Therefore,

$$\mathbb{P}\big(\text{absorption in bin } k\big) \;=\; \mathbb{E}\big[P_k(0)\big] \;=\; \sum_{i \in \mathcal{I}_k} p_i(0),$$

and the Born weights add across degenerate channels.

Continuous spectra.

For a continuum of channels (outcome space $(\mathcal{Y}, \mathcal{B})$), approximate by partitions $\mathcal{P}_n = \{A_j^{(n)}\}$ with mesh $\to 0$ and define $p_j^{(n)}(0)$ as initial overlaps for $A_j^{(n)}$. The absorption measure $\mu^{(n)} := \sum_j \mathbb{P}(Y \in A_j^{(n)})\, \delta_{A_j^{(n)}}$ converges weakly to a probability measure μ on $(\mathcal{Y}, \mathcal{B})$ with density determined by the $L^2(\Gamma)$ overlap field (the Radon–Nikodym derivative is the limit of normalized $S_j^{(n)}$). Hence Born probabilities extend to continuous outcomes by a standard projective limit [8].

POVMs via Naimark dilation.

Let $\{E_k\}_{k=1}^K$ be a POVM on the microscopic Hilbert space. Realize it as a projective measurement $\{P_\ell\}$ on an enlarged ancilla+system space via Naimark's dilation [68,77]. In the CFT interface picture, add ancilla alignment channels $\{\tilde{\Gamma}_\ell\}$ coupled unitarily to the system before the boundary layer, so that each E_k corresponds to a union of orthogonal projective channels in the dilation. By the degeneracy argument above,

$$\mathbb{P}(\text{outcome } k) \;=\; \sum_{\ell \in \mathcal{J}_k} p_\ell(0) \;=\; \mathrm{Tr}\big(\rho\, E_k\big),$$

with ρ the density operator induced by the preparation (pure state: $\rho = |\psi\rangle\langle\psi|$).

8.3. Basis invariance and Gleason-Type Constraints

We now justify that quadratic (Born) dependence is *forced* by natural consistency axioms once outcomes are identified with orthogonal apparatus channels.

Definition 25 (Frame function on projectors)**.** Let $\mathcal{H}$ be a complex Hilbert space of dimension ≥ 3. A map P assigning probabilities to rank–one orthogonal projectors $P = |\varphi\rangle\langle\varphi|$ is a *frame function* if:

 doi:10.20944/preprints202508.2056.v1

(F1) (*Normalization and additivity*) For every orthonormal basis $\{\varphi_i\}$, $\sum_i \mathsf{P}(|\varphi_i\rangle\langle\varphi_i|) = 1$.
(F2) (*Noncontextuality*) $\mathsf{P}(P)$ depends only on P, not on the basis in which P is embedded.
(F3) (*Measurability/continuity*) P is Borel measurable on the unit sphere (or continuous).

Proposition 26 (Gleason-type constraint)**.** *Assume* (F1)–(F3). *Then there exists a unique density operator* ρ *such that*

$$\mathsf{P}(P) \;=\; \mathrm{Tr}(\rho\, P) \qquad \textit{for all rank–one projectors } P.$$

In particular, for pure preparations $\rho = |\psi\rangle\langle\psi|$, *one has* $\mathsf{P}(|\varphi\rangle\langle\varphi|) = |\langle\varphi,\psi\rangle|^2$.

Proof sketch. This is Gleason's theorem [41] for complex Hilbert spaces of dimension ≥ 3. In our setting, (F1) is frame additivity across apparatus eigen–decompositions; (F2) is basis invariance of the interface (Section 2); (F3) follows from continuity of overlaps. Thus the only consistent assignment is quadratic. For 2–dimensional systems, add an ancilla and use Naimark dilation (or continuity and nontrivial mixing) to extend the result [11]. □

Synthesis.

The martingale/absorption derivation fixes the single–trial law to be $p_i(0)$ in any apparatus basis. Proposition 26 shows that basis–independent, additive assignments over orthogonal channels must be quadratic; therefore identifying $p_i(0) = |c_i|^2$ (Section 2) is not merely convenient but *forced* by structural consistency. The stability estimate in Theorem 8.1 then quantifies deviations under realistic imperfections.

9. Experimental and Numerical Signatures

This section discusses measurable and simulable consequences of the alignment picture. We give parameter scalings for alignment/fixation times, show how to bound residual drift b^* by weak monitoring at the interface, and outline a simulation suggestion at both microscopic (chronon) and macroscopic (simplex SDE) levels.

Alignment and fixation timescales; dependence on η *and* β

Two stages control the time to a recorded outcome.

(i) Deterministic alignment in the boundary layer.

Let $\Phi(t)$ evolve by the deterministic gradient flow associated with the interface free energy $\mathcal{F}_\eta$ (zero noise limit of (8)–(9)). Write $\Phi^\star$ for the unique minimizer in the boundary layer and measure deviations in an H^1–norm adapted to the boundary metric.

Theorem 9.1 (Exponential alignment)**.** *Assume* $\mathcal{F}_\eta$ *is* λ*–convex in a neighborhood of* $\Phi^\star$ *and that the linearized operator at* $\Phi^\star$ *has spectral gap* $\gamma = \gamma(\eta, \kappa, \lambda_{\mathrm{eff}}, m^2_{\mathrm{eff}}) > 0$ *with respect to the boundary* H^1 *inner product. Then there exists* $C \geq 1$ *such that for all sufficiently small neighborhoods,*

$$\|\Phi(t) - \Phi^\star\|_{H^1(bdy)} \;\leq\; C\, e^{-\gamma t}\, \|\Phi(0) - \Phi^\star\|_{H^1(bdy)}. \tag{26}$$

Consequently, the time to enter an H^1*–ball of radius* ε *satisfies*

$$\tau_{\mathrm{det}}(\varepsilon) \;\asymp\; \gamma^{-1}\, \log \frac{\|\Phi(0) - \Phi^\star\|_{H^1}}{\varepsilon}, \tag{27}$$

with γ *increasing monotonically in the boundary penalty* η *and decreasing with temperature* β^{-1} *(via effective convexity).*

 doi:10.20944/preprints202508.2056.v1

(ii) Stochastic fixation on the outcome simplex.

After alignment, the overlaps $p(t)$ follow the Wright–Fisher diffusion on Δ^{m-1} with intensity $\alpha > 0$ (Theorem 3.1). Let $\tau := \inf\{t \geq 0 : p(t) \in \{e_1, \ldots, e_m\}\}$. Then

$$\frac{c_1}{\alpha} H(p^\star) \;\leq\; \mathbb{E}[\tau \mid p(0) = p^\star] \;\leq\; \frac{c_2}{\alpha} H(p^\star), \qquad H(p) := -\sum_{i=1}^{m} p_i \log p_i, \tag{28}$$

for constants c_1, c_2 depending only on m [33,43]; in the two–channel case [54],

$$\mathbb{E}[\tau \mid p(0) = p] \;=\; -\frac{2}{\alpha}\big[p \log p + (1-p)\log(1-p)\big]. \tag{29}$$

The diffusion intensity admits a Green–Kubo representation in terms of boundary alignment currents $J_i(t)$:

$$\alpha \;=\; \frac{2}{\mathrm{Area}_\gamma(\Gamma)} \int_0^\infty \sum_{i=1}^{m} \mathrm{Cov}_{\mu_{\beta,\eta}}\big(J_i(t), J_i(0)\big)\, \mathrm{d}t, \tag{30}$$

which scales as

$$\alpha \;\asymp\; \frac{\beta^{-1}\, \mathsf{Mob}_\Gamma(\eta)}{\mathrm{Area}_\gamma(\Gamma)}\, \Xi(\kappa, \lambda_{\mathrm{eff}}), \tag{31}$$

with $\mathsf{Mob}_\Gamma(\eta)$ the effective boundary mobility (increasing with η) and Ξ a dimensionless stiffness factor depending smoothly on $(\kappa, \lambda_{\mathrm{eff}})$ [59].

Combining (27) and (28) gives the lock–in time

$$\tau_{\mathrm{lock}} \;\approx\; \tau_{\mathrm{det}}(\varepsilon) \;+\; \mathbb{E}[\tau \mid p(0) = p^\star] \;\sim\; \gamma^{-1} \log \varepsilon^{-1} \;+\; \frac{C}{\alpha} H(p^\star), \tag{32}$$

decreasing with stronger coupling (larger η) and colder boundary (larger β).

Drift Constraints from Weak Monitoring

Residual symmetry breaking (finite η, geometry, temperature) produces a small effective drift $b^*(p)$ in the simplex dynamics, biasing outcome probabilities (Theorem 8.1). We outline an experiment to bound $\|b^*\|_\infty$ by weakly monitoring the overlaps before absorption.

Protocol.

Prepare many identical runs with the same $p^\star$ and *weakly interrogate* the interface at a cadence faster than fixation yet weak enough not to alter α at leading order. From short increments $\Delta p_i = p_i(t + \Delta t) - p_i(t)$ collected away from the boundary, define

$$\widehat{b}_i \;=\; \frac{1}{T} \sum_{k=1}^{T/\Delta t} \frac{\Delta p_i^{(k)}}{\Delta t}, \qquad \widehat{v}_i \;\approx\; \alpha\, p_i(1-p_i)$$

(the latter from sample variances).

Sample complexity and bound.

Under the neutral model, $\mathbb{E}[\Delta p_i] = 0$ and $\mathrm{Var}(\Delta p_i) \approx \alpha\, p_i(1-p_i)\, \Delta t$. A Bernstein/Freedman inequality [36,89] yields

$$\mathbb{P}\Big(|\widehat{b}_i - b_i^*| \geq \epsilon \Big) \;\leq\; 2\exp\!\left(-\frac{c\, \epsilon^2\, T}{\alpha\, p_i(1-p_i)} \right), \tag{33}$$

 doi:10.20944/preprints202508.2056.v1

for a universal $c > 0$, where $\overline{p_i(1-p_i)}$ is the time average along the run (bounded by $1/4$). To certify $|b_i^*| \le \epsilon$ with confidence $1-\delta$ it suffices that

$$T \gtrsim \frac{\alpha}{c\,\epsilon^2} \log\frac{2}{\delta}. \tag{34}$$

A union bound over $i = 1, \dots, m$ gives a uniform constraint on $\|b^*\|_\infty$, which feeds into Theorem 8.1 to bound deviations from Born weights.

Numerical Method: Chronon Lattice and Simplex SDE

We recommend a two–tier simulation strategy.

Tier I: microscopic chronon simulation (boundary layer).

- Discretize U_Γ into a lattice of spacing ℓ_{uv} and simulate the overdamped Langevin dynamics (8)–(9) (or their discrete counterparts) with parameters $(\kappa, \lambda_{\text{eff}}, m_{\text{eff}}^2, \eta, \beta)$ using standard Langevin integrators [83].
- Measure *alignment currents* $J_i(t) = \dot{S}_i(t) - \mathbb{E}[\dot{S}_i \mid p]$ and estimate α via the Green–Kubo integral (30) (truncate at a few mixing times) [59].
- Validate detailed balance numerically (time–reversal tests [14]) and estimate the small drift b^* by conditional averages; symmetry implies $b^* \approx 0$ within tolerance in the symmetric case.
- Perform finite–size scaling in η and β to map $\alpha(\eta, \beta)$ and the deterministic gap $\gamma(\eta, \cdot)$ (from relaxation of $\mathcal{F}_\eta$).

Tier II: macroscopic SDE on the simplex.

- Simulate the Wright–Fisher SDE (14) with the measured α, using an Euler–Maruyama scheme [57] with projection to the simplex interior and absorbing at the vertices (or a square–root factorization for exact covariance).
- Verify the martingale property $\mathbb{E}[p_i(t)] \equiv p_i(0)$ and the absorption law $\mathbb{P}(p(\tau) = e_i) = p_i(0)$ across a grid of initial conditions.
- Add a small drift b^* and perturb $a(p)$ as indicated by the chronon estimates; quantify deviations from Born via Theorem 8.1.
- For repeated trials, generate empirical frequency histograms and compare with the Sanov LDP (Theorem 7.1): plot $-\frac{1}{N}\log \mathbb{P}(\hat{f}_N \approx q)$ against $D(q\|p^\star)$ [19].

Reporting and diagnostics.

Key plots include: (i) τ_{det} vs. η and β; (ii) α vs. η (log–log to expose scaling); (iii) fixation time distributions vs. $H(p^\star)$ compared with (28)–(29); (iv) bounds on $\|b^*\|_\infty$ from (34); (v) LDP verification by linearity against $D(q\|p^\star)$.

Experimental readout.

In atom/photonic interferometry or solid–state platforms with spatially resolved detectors, η can be tuned by coupling (aperture, impedance matching); β by temperature/cryogenics; and $\text{Area}_\gamma(\Gamma_i)$ by detector geometry. Weak monitoring of overlaps $p_i(t)$ can be implemented by low–gain probe pulses or non–destructive readouts calibrated to leave α invariant to first order. Expected signatures: faster lock–in with stronger coupling (decreasing τ_{lock}) and Born–consistent outcome frequencies with deviations bounded by Theorem 8.1.

10. Discussion

Synthesis.

We have given a coordinated derivation of Born probabilities in the chronon framework along three complementary paths: (i) a *martingale/absorption* argument on the outcome simplex (Sections 3–

 doi:10.20944/preprints202508.2056.v1

4), where detailed balance and channel symmetry force zero drift and optional stopping identifies single–shot outcome weights with initial overlaps (cf. [31]); (ii) a *hydrodynamic limit* from microscopic chronon dynamics (Section 6), which yields the Wright–Fisher diffusion for the overlap vector and pins down the diffusion intensity by a boundary Green–Kubo formula [59]; (iii) a *large–deviation* analysis of empirical frequencies (Section 7), establishing that fluctuations concentrate exponentially at the Born vector with rate $I(q) = D(q\|p^\star)$ [19]. Robustness bounds (Section 8) quantify deviations induced by finite interface strength, temperature, geometric asymmetry, and small residual drifts.

Operational comparison to other approaches.

Collapse models (e.g. GRW/CSL [4]) postulate stochastic modifications of the Schrödinger equation; by contrast, stochasticity here is *classical*, confined to the apparatus boundary layer, and enters only through the chronon alignment dynamics. Unitary quantum evolution for the microscopic degrees of freedom is not modified; definite outcomes arise by absorbing fixation of the overlap diffusion. *Quantum trajectories* and continuous measurement theories [94] also produce martingale structures for conditional state components, typically from measurement back–action; our derivation replaces back–action dynamics with *boundary–induced* alignment under detailed balance, then projects onto overlaps that obey a neutral diffusion on the simplex. *QBist/epistemic* accounts interpret Born weights as degrees of belief; in contrast, the present probabilities are *frequencies* of absorption events in a single–world dynamics, grounded in Dirichlet problems for a diffusion obtained from a hydrodynamic limit. *Consistent histories* [38] identifies decoherent sets of histories and assigns probabilities via a decoherence functional; our construction is effectively a consistent–histories reduction on the interface coarse–graining, with the additional structure that the coarse–grained stochastic dynamics is explicitly identified and reversible with respect to a Gibbs measure. Finally, unlike *branching/many–worlds*, the alignment plus absorption yields exclusivity via absorbing vertices on Δ^{m-1}, not by postulated multiplicity of outcomes.

Conceptual economy.

Three structural ingredients suffice: (i) a stabilized apparatus foliation and unit–norm timelike Φ_A; (ii) a reversible noisy alignment dynamics satisfying fluctuation–dissipation [14]; (iii) orthogonal channelization of the interface and projection to overlaps. No additional probability postulates are needed. Gleason–type constraints (Proposition 26; cf. [41]) then show that the quadratic form is not merely convenient but *forced* by basis–invariant additivity over orthogonal channels.

Scope and limitations.

The diffusion limit rests on mixing/chaos hypotheses for the boundary layer and on time–scale separation (Assumptions 16, 19). These are natural for short–range ferromagnetic chronon couplings and sufficiently strong interface pinning, but require refinement for long–range interactions, glassy disorder, or nonlocal mobilities. The Wright–Fisher covariance and zero drift arise from channel symmetry and detailed balance; small violations introduce controlled errors (Theorem 8.1), yet a full classification of admissible symmetry breakings that *still* yield Born weights remains open. The present treatment is classical on the apparatus side; while this matches the coarse–grained aim, it leaves open the back–reaction of quantized Φ fluctuations (below).

Open problems.

We list directions where further mathematical development is needed.

- **Quantization of Φ and constraint algebra.** Develop a constraint–consistent quantum theory of the chronon field Φ^μ (canonical or BRST), and analyze how quantum fluctuations of Φ modify the boundary fluctuation–dissipation relation and the overlap diffusion coefficients.
- **Nonlocal couplings and memory.** Extend the hydrodynamic limit to kernels with finite tails (retarded or spatially nonlocal mobilities), including colored boundary noise [74]. Identify

 doi:10.20944/preprints202508.2056.v1

conditions under which the projected process on Δ^{m-1} remains Markov, or quantify controllable non–Markovian corrections and their effect on fixation probabilities.

- **Beyond second–order dynamics.** Analyze the strictly hyperbolic (damped wave) class (H) at the stochastic level in curved backgrounds, derive its diffusive limit at the interface, and compare transport coefficients with the overdamped class (P).
- **Sequential and incompatible measurements.** For a sequence of measurements with noncommuting channel decompositions, characterize the joint process on the product of simplices and show that Lüders' rule emerges in the chronon–alignment picture.
- **Entangled preparations and multipartite interfaces.** Extend the analysis to two or more spatially separated interfaces coupled to a common preparation, track the joint overlap diffusion, and derive Tsirelson–bound–consistent correlations without superluminal signalling.
- **Sharp rates and finite–size corrections.** Prove quantitative rates for the hydrodynamic convergence (Section 6) and for the Sanov LDP under α–mixing (Theorem 7.1), including explicit constants in terms of $(\eta, \beta, \kappa, \lambda_{\text{eff}})$ and geometry.

Empirical outlook.

The alignment picture yields concrete scalings: the lock–in time τ_{lock} decreases with interface strength η and inverse temperature β, and fixation times scale as $H(p^\star)/\alpha$ (Eqns. (28)–(31)). Weak monitoring of overlaps provides direct bounds on residual drift (Eqns. (33)–(34)), which translate into quantitative bounds on deviations from Born via Theorem 8.1. These signatures are accessible in interferometric, photonic, and solid–state platforms with tunable coupling and temperature.

Within CFT, Born probabilities arise as absorption probabilities of a neutral diffusion on the outcome simplex, itself the hydrodynamic limit of reversible noisy alignment at the apparatus boundary. The derivation is operational, basis–invariant, and robust to realistic limitations. Completing the quantum treatment of Φ, extending to nonlocal dynamics, and refining rates will test the universality of this mechanism and further integrate it with covariant emergent–spacetime programs.

11. Conclusion

We have given a complete, operational derivation of the Born rule within the chronon framework for measurement as boundary–induced alignment. At the level of effective observables, we proved that the alignment–overlap vector $p(t)$ on the outcome simplex Δ^{m-1} arises as the hydrodynamic limit of reversible noisy alignment in the boundary layer and converges to a neutral Wright–Fisher diffusion (Theorem 3.1; cf. [31]). Channel symmetry and detailed balance enforce zero drift, so each coordinate $p_i(t)$ is a martingale up to fixation; optional stopping then identifies single–shot outcome probabilities with initial overlaps, yielding the Born weights (Theorem 4.1, cf. martingale methods in [28]). On repeated trials, empirical frequencies obey a Sanov large–deviation principle with rate $I(q) = D(q\|p^\star)$ minimized at the Born vector (Theorem 7.1; see [19]). Quantitative robustness was established against finite interface strength, temperature, and small asymmetries, with explicit error bounds on deviations from Born probabilities (Theorem 8.1). Degeneracies, continuous spectra, and POVMs were handled by grouping, approximation, and Naimark dilation (cf. [68]), while basis–invariant additivity forces the quadratic law via a Gleason–type constraint (Proposition 26; cf. [41]).

A practical path to a chronon–based probability law.

The results here supply a pipeline from device parameters to outcome statistics: (i) calibrate the deterministic alignment gap and the boundary diffusion intensity α from relaxation and fluctuation measurements (Green–Kubo formula, Eq. (30); cf. [59]); (ii) bound residual drifts b^* by weak monitoring of overlaps pre–fixation (Eqs. (33)–(34)); (iii) predict fixation times and outcome probabilities via the simplex SDE with absorption and apply the robustness bound (25). This yields a chronon–level, device–controllable account of Born statistics without additional probabilistic postulates.

 doi:10.20944/preprints202508.2056.v1

Next steps.

Three most pressing directions need further development:

- **Hydrodynamic program to completion.** Strengthen Theorem 6.1 to full (non–sketch) proofs with explicit rates in terms of $(\eta, \beta, \kappa, \lambda_{\text{eff}})$ and geometry; treat long–range kernels and colored noise while preserving Markovian limits or quantifying controlled memory corrections (cf. [74]).
- **Tighter robustness and sequential protocols.** Sharpen constants in Theorem 8.1; analyze cascaded and incompatible measurements (product simplices), deriving Lüders' rule and quantifying composition errors from residual drift (cf. [12]).
- **Experimental tests.** Measure $\alpha(\eta, \beta)$ and lock–in times (Eqs. (28)–(31)) across tunable interfaces; implement weak–monitoring bounds on b^* and verify Sanov scaling for frequency histograms. Extending to multipartite interfaces will test nonlocal correlations against Tsirelson bounds [15] within the alignment picture.

We have shown that, Born probabilities emerge here as fixation probabilities of a neutral diffusion that is itself the macroscopic shadow of reversible boundary alignment. This closes the conceptual loop between chronon microdynamics, apparatus geometry, and quantum outcome statistics, and provides a concrete route to broaden, test, and ultimately quantize the chronon description in future work.

Interpretational summary.

Chronon Field Theory provides a unified account of outcome definiteness and Born statistics grounded in geometric field interactions. The alignment field mediates coupling between a microscopic quantum system and a macroscopic apparatus with stabilized eigen–domains. Under stochastic fluctuations at the measurement interface, the system probabilistically aligns with one domain, modeled as absorption in the outcome simplex. This structure yields definite outcomes without invoking nonlocality or wavefunction collapse, and derives Born weights as hitting probabilities.

Engineered Definiteness.

A final reflection concerns the status of definiteness itself. In standard accounts, the system is thought to *collapse* into one of its own eigenstates, as though the definite outcome were already latent in the microscopic degrees of freedom. The present analysis suggests a deeper view: the chronon field Φ of the microscopic system is not classically aligned, and the measured classical features must be *engineered* by the detector. Definiteness arises only through coupling to an apparatus whose geometry provides stabilized eigen–domains. What the observer records as a single, definite outcome is thus the reflection of the system's potential structure in the engineered alignment channels of the measuring device. In this sense, the apparatus does not merely reveal but actively *constructs* the conditions under which the Born rule applies. Such a perspective is consistent with the operational content of textbook quantum mechanics, but reframes it: measurement outcomes are not passively discovered, but dynamically produced by the stochastic geometry of system–apparatus interaction.

Appendix L Existence of Apparatus Eigen–Domains

This appendix provides a formal justification for the existence of a finite family of apparatus eigen–domains along the measurement interface Γ in Chronon Field Theory (ChFT). These domains play a central role in defining the alignment overlap vector $p(t)$ and in formulating the measurement dynamics as a stochastic absorption process on the outcome simplex Δ_{m-1}.

Proposition A27 (Existence of Apparatus Eigen–Domains). *Let $\mathcal{A} \subset \mathbb{R}^4$ denote a macroscopic apparatus region with stabilized coarse–grained field $\Phi^{\mu}_{\mathcal{A}}$, assumed to be future–directed, unit–norm, and twist–free, and let $\Gamma = \partial\Omega \cap \mathcal{A}$ denote the measurement interface. Then, under the unit–norm constraint and the alignment-based interface energy coupling, the boundary region Γ admits a finite partition into disjoint open subsets*

$$\Gamma = \bigsqcup_{i=1}^{m} \Gamma_i,$$

 doi:10.20944/preprints202508.2056.v1

called apparatus eigen–domains, *with the following properties:*

1. *Each* Γ_i *corresponds to a distinct, locally stable alignment configuration of the chronon field* Φ^μ *with the apparatus field* $\Phi^\mu_{\mathcal{A}}$*;*
2. *The alignment energy* $S_i(\Phi)$*, defined over* Γ_i *via*

$$S_i(\Phi) = \int_{\Gamma_i} f\Big(-g_{\mu\nu}\Phi^\mu_A(x)\Phi^\nu(x)\Big)\, d\sigma_\gamma(x),$$

   is maximized when Φ^μ *aligns with the dominant direction in* Γ_i*;*
3. *The number of such eigen–domains* m *is finite, determined by coarse–graining resolution and the topological stability of alignment basins under boundary noise;*
4. *The overlap vector* $p(0) = (p_1(0), \ldots, p_m(0))$ *constructed from the* $S_i(\Phi)$ *defines the initial condition for the stochastic alignment process (Definition 7).*

These domains correspond to the measurable outcome channels of the apparatus and provide the geometric basis for stochastic absorption and outcome selection in Chronon Field Theory.

Proof sketch. We outline why a finite family of stable alignment basins (eigen–domains) $\{\Gamma_i\}_{i=1}^m$ must exist along the measurement interface Γ under the assumptions of the CFT model.

Step 1: Stabilization of $\Phi^\mu_{\mathcal{A}}$.

The apparatus field $\Phi^\mu_{\mathcal{A}}$ is assumed to be stabilized on macroscopic scales (Definition 1). It is approximately constant in both norm and direction within localized neighborhoods on Γ, enabling local alignment analysis.

Step 2: Variational structure of alignment energy.

The alignment energy density is given by a function $f(s)$ of the inner product $s(x) = -g_{\mu\nu}\Phi^\mu_A(x)\Phi^\nu(x)$, which is maximized when the fields are aligned. With the choice $f(s) = s^2$ and the unit–norm constraint on Φ^μ, the energy functional over Γ has local minima corresponding to aligned configurations.

The companion paper [63] establishes that under a global unit–norm constraint, the chronon field selects Lorentzian signature and prefers alignment with stable time-like directions. These preferred directions arise as energetic minima under the boundary coupling.

Step 3: Domain formation via local minima.

Due to coarse–graining and microscopic fluctuations, Γ is not globally homogeneous. Small inhomogeneities in $\Phi^\mu_{\mathcal{A}}$, local curvature, or interface imperfections create multiple distinct local minima in the alignment energy landscape. Each such minimum corresponds to a region Γ_i where a specific alignment direction dominates.

The field Φ^μ tends to align stochastically with one of these regions under the boundary dynamics, producing a discrete set of alignment basins—i.e., eigen–domains.

Step 4: Finiteness and measurability.

Because $\Phi^\mu_{\mathcal{A}}$ is smooth at the macroscopic scale, only a finite number of such domains can arise within the spatial resolution of the apparatus. Each Γ_i is an open measurable subset of Γ, and the full boundary decomposes as a finite disjoint union $\Gamma = \bigsqcup_i \Gamma_i$.

Conclusion.

Therefore, a finite collection of eigen–domains $\{\Gamma_i\}$ emerges from the variational dynamics and stabilized apparatus structure. These domains support distinct alignment channels and provide the geometric basis for the stochastic absorption process used in deriving the Born rule. □

 doi:10.20944/preprints202508.2056.v1

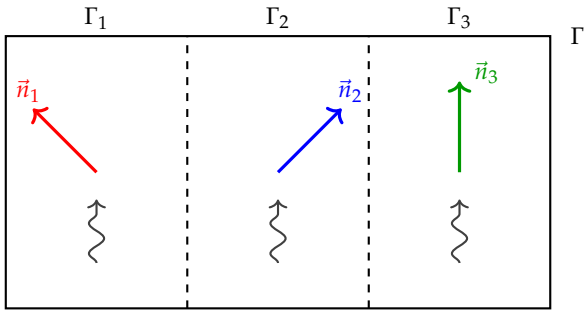

Figure A3. Schematic representation of the measurement interface Γ, partitioned into three eigen–domains Γ_1, Γ_2, and Γ_3, each corresponding to a locally stabilized alignment direction of the apparatus field, denoted $\vec{n}_1$, $\vec{n}_2$, and $\vec{n}_3$. These coarse–grained domains emerge from the variational coupling between the system and measurement apparatus, and support distinct alignment channels through which the system's state becomes entangled with macroscopic pointer configurations. The wavy arrows indicate domain–localized stochastic absorption events, representing the probabilistic registration of measurement outcomes and forming the geometric substrate for Born rule derivation.

Remark A28. See Figure A3. When the microsystem undergoes stochastic absorption within one of the eigen–domains—say, Γ_3—this domain becomes the site of measurement registration, establishing a definite alignment with the corresponding apparatus direction $\vec{n}_3$. The remaining domains Γ_1 and Γ_2, though still present as structural components of the apparatus interface, become dynamically suppressed. That is, they no longer carry amplitude in the post-measurement state and cease to participate in the entangled system–apparatus configuration. From the perspective of the variational dynamics, these domains no longer contribute to the extremal action paths and are effectively bypassed in the realized outcome. In this sense, they become dynamically empty, providing no support for further absorption events once the outcome is registered in Γ_3.

Appendix M SDE on the Simplex with Absorbing Faces

We collect well–posedness, boundary classification, and basic identities for Itô diffusions on the probability simplex

$$\Delta^{m-1} := \Big\{ p = (p_1, \dots, p_m) \in [0,1]^m : \sum_{i=1}^{m} p_i = 1 \Big\}, \qquad m \geq 2,$$

with focus on the neutral (zero–drift) Wright–Fisher covariance and *absorbing* boundary at the vertices $\{e_i\}_{i=1}^m$; see, e.g., [31,33,54].

Generators, SDE representations, and invariance

We consider second–order operators on $C^2(\mathrm{ri}(\Delta^{m-1}))$ of the form

$$\mathcal{L}f(p) = \frac{1}{2} \sum_{i,j=1}^{m} a_{ij}(p)\, \partial_i \partial_j f(p) + \sum_{i=1}^{m} b_i(p)\, \partial_i f(p), \tag{A35}$$

with the Wright–Fisher covariance

$$a_{ij}(p) = \alpha \Big(\delta_{ij}\, p_i - p_i p_j \Big), \qquad \alpha > 0, \tag{A36}$$

and drift $b : \Delta^{m-1} \to \mathbb{R}^m$ tangent to Δ^{m-1}, i.e. $\sum_i b_i(p) = 0$ for all p. The form (A36) is canonical for neutral multi-allele Wright–Fisher limits [31,33].

 doi:10.20944/preprints202508.2056.v1

Proposition A29 (SDE representation and invariance). *Let $W = (W_1, \dots, W_m)$ be an m–dimensional standard Brownian motion. Consider the Itô SDE on $\mathbb{R}^m$*

$$\mathrm{d}p(t) \;=\; b\big(p(t)\big)\,\mathrm{d}t \;+\; \sqrt{\alpha}\,\Big(I - p(t)\,\mathbf{1}^\top\Big)\,\sqrt{\mathrm{Diag}\big(p(t)\big)}\,\mathrm{d}W(t), \tag{A37}$$

started at $p(0) \in \Delta^{m-1}$, where $\mathbf{1} = (1, \dots, 1)^\top$ and $\sqrt{\mathrm{Diag}(p)}$ is the diagonal matrix with entries $\sqrt{p_i}$. Then $\sum_i p_i(t) \equiv 1$, $p_i(t) \geq 0$ for all i, and the formal generator on $C^2(\mathrm{ri}(\Delta^{m-1}))$ is (A35)–(A36). *(Cf. [31]; see also [53, §5.5].)*

Proof. The noise coefficient is $\sigma(p) := \sqrt{\alpha}(I - p\mathbf{1}^\top)\sqrt{\mathrm{Diag}(p)}$. Since $\mathbf{1}^\top(I - p\mathbf{1}^\top) = \mathbf{1}^\top - \mathbf{1}^\top p\,\mathbf{1}^\top = 0$, Itô yields $\mathrm{d}\sum_i p_i \;=\; \sum_i b_i\,\mathrm{d}t + \mathbf{1}^\top\sigma\,\mathrm{d}W \;=\; 0$ (tangency of b), hence invariance of the hyperplane. Moreover,

$$\sigma(p)\sigma(p)^\top \;=\; \alpha\,(I - p\mathbf{1}^\top)\,\mathrm{Diag}(p)\,(I - \mathbf{1}p^\top) \;=\; \alpha\big(\mathrm{Diag}(p) - pp^\top\big),$$

which gives (A36). Nonnegativity follows from the degeneracy of σ at $\partial\Delta^{m-1}$; cf. [31, Prop. 10.1.1]. □

Well–posedness and boundary classification

Because $a(p)$ is only positive semidefinite and degenerates at $\partial\Delta^{m-1}$, strong well-posedness may fail globally; the right framework is the *martingale problem* with boundary conditions [31,86].

Definition A30 (Martingale problem with absorbing boundary). Let $C_c^2(\mathrm{ri}(\Delta^{m-1}))$ be smooth functions compactly supported in the interior. A probability measure $\mathbb{P}$ on $D([0,\infty), \Delta^{m-1})$ solves the martingale problem for $(\mathcal{L}, \mu_0)$ with *absorbing boundary at vertices* if $p(0) \sim \mu_0$ and for all $f \in C_c^2(\mathrm{ri}(\Delta^{m-1}))$,

$$M_f(t) \;:=\; f\big(p(t)\big) - f\big(p(0)\big) - \int_0^t \mathcal{L}f\big(p(s)\big)\,\mathrm{d}s$$

is a $\mathbb{P}$–martingale, and if p is absorbed on first hitting any vertex e_i: $p(t) = e_i$ for all $t \geq \tau$ whenever $p(\tau) = e_i$; cf. [86, Ch. 6].

Theorem M.1 (Existence and uniqueness in law). *Assume b is continuous, locally Lipschitz on $\mathrm{ri}(\Delta^{m-1})$, tangent ($\sum_i b_i \equiv 0$), and at most linear growth. Then for each initial law μ_0 on Δ^{m-1}, the martingale problem for* (A35)–(A36) *with absorbing vertices is well–posed: there exists a solution and it is unique in law. Moreover, the solution coincides with the weak solution of the SDE* (A37)*, absorbed at the vertices [31,86].*

Remark A31 (Reflecting vs. absorbing faces; mutation drift). Adding a *parent–independent mutation* drift

$$b_i^{(\theta)}(p) \;=\; \frac{\alpha}{2}\,(\theta_i - \theta\,p_i), \qquad \theta_i \geq 0, \quad \theta := \sum_{j=1}^m \theta_j, \tag{A38}$$

changes the boundary classification: if $\theta_i > 0$ for all i, faces become *entrance* (no absorption) and the stationary law is $\mathrm{Dir}(\theta_1, \dots, \theta_m)$; if $\theta_i = 0$ for all i, faces are *absorbing* and no stationary distribution exists [33,54]. Our setting corresponds to $\theta \equiv 0$.

Conservation, martingales, and absorption times

Proposition A32 (Conservation laws and coordinate martingales). *For the neutral case $b \equiv 0$:*

1. *$\sum_i p_i(t) \equiv 1$ for all t.*
2. *Each coordinate $p_i(t)$ is a bounded martingale up to the absorption time $\tau := \inf\{t : p(t) \in \{e_1, \dots, e_m\}\}$, hence $\mathbb{E}[p_i(t \wedge \tau)] = \mathbb{E}[p_i(0)]$ and $\mathbb{E}[\mathbf{1}_{\{p(\tau) = e_i\}}] = \mathbb{E}[p_i(0)]$ [31].*

Theorem M.2 (Absorption in finite time; estimates). *In the neutral, absorbing case $b \equiv 0$, the first hitting time τ of the vertex set is a.s. finite with $\mathbb{E}[\tau] < \infty$. Moreover, there exist $0 < c_1 \leq c_2 < \infty$ depending only on m such that*

$$\frac{c_1}{\alpha}\,H\big(p(0)\big) \;\leq\; \mathbb{E}[\tau] \;\leq\; \frac{c_2}{\alpha}\,H\big(p(0)\big), \qquad H(p) := -\sum_{i=1}^m p_i \log p_i. \tag{A39}$$

 doi:10.20944/preprints202508.2056.v1

For $m = 2$,

$$\mathbb{E}[\tau \mid p_1(0) = x] \;=\; -\frac{2}{\alpha}\big[x\log x + (1-x)\log(1-x)\big]. \tag{A40}$$

Proof sketch. For $m = 2$, (A40) follows from the standard scale–speed calculation for one-dimensional Wright–Fisher diffusions [33, §4.6]; see also [54, §15]. For $m \geq 3$, Lyapunov functions such as $V(p) = \sum_i p_i(1-p_i)$ or $V(p) = H(p)$ yield $\mathcal{L}V \leq -c\sum_{i<j} p_i p_j$ away from vertices; Foster–Lyapunov arguments give a.s. absorption and the bounds (A39) [66, Ch. 7]. □

Reflecting faces and stationary Dirichlet laws

Proposition A33 (Stationarity under mutation/inward drift). *Let $b = b^{(\theta)}$ be as in (A38) with $\theta_i > 0$ for all i. Then the martingale problem on Δ^{m-1} with* no absorption *is well–posed and admits the reversible stationary distribution* $\mathrm{Dir}(\theta_1, \ldots, \theta_m)$ *[31,33]. In particular, for any $f \in C^2(\Delta^{m-1})$,*

$$\int_{\Delta^{m-1}} \mathcal{L}f(p)\,\mathrm{Dir}(\theta)(\mathrm{d}p) \;=\; 0.$$

Notes on strong solutions and pathwise uniqueness

The diffusion coefficient in (A37) is only Hölder $1/2$ and vanishes at $\partial\Delta^{m-1}$, so global pathwise uniqueness need not hold; cf. the Yamada–Watanabe criteria [95]. On each compact subset of $\mathrm{ri}(\Delta^{m-1})$ coefficients are locally Lipschitz, yielding strong well–posedness up to the (random) hitting time of the boundary [53, §5.2]. For our purposes, uniqueness in law via the martingale problem (Theorem M.1) suffices [86].

Summary and comparison

- The neutral Wright–Fisher diffusion (A37) with $b \equiv 0$ is well–posed on Δ^{m-1} with absorbing vertices, preserves the simplex, and absorbs in finite time almost surely [31,33].
- Adding parent–independent mutation (A38) converts faces from absorbing to entrance and yields a Dirichlet stationary law [33,54].
- Our main text uses the neutral, absorbing case to represent selection of a unique outcome by fixation at a vertex, with absorption probabilities given by initial coordinates (martingale/optional stopping) [31].

Appendix N Optional Stopping: Uniform Integrability and Hitting Times

This appendix states the uniform–integrability (UI) criteria and a version of Doob's optional stopping theorem used in Section 4, and supplies complete proofs of Proposition 17, Theorem 4.1, and Lemma 18 for the Wright–Fisher diffusion on the simplex with absorbing vertices (Appendix M). Standard background can be found in [26,53,81,93].

Uniform integrability and optional stopping

Definition A34 (Uniform integrability). A family $\mathcal{F} \subset L^1(\Omega, \mathcal{F}, \mathbb{P})$ is *uniformly integrable* if

$$\lim_{K\to\infty} \sup_{X\in\mathcal{F}} \mathbb{E}\big[\,|X|\,\mathbf{1}_{\{|X|>K\}}\,\big] \;=\; 0.$$

A càdlàg martingale $(M_t)_{t\geq 0}$ is *uniformly integrable* if $\{M_t : t \geq 0\}$ is UI [81, §III.3].

Lemma A35 (Bounded martingales are UI). *If $(M_t)_{t\geq 0}$ is a martingale with $|M_t| \leq K$ almost surely for all t, then $\{M_t : t \geq 0\}$ is uniformly integrable [93, Prop. 10.10].*

Proof. For any $K' > K$, $\mathbb{E}[|M_t|\mathbf{1}_{\{|M_t|>K'\}}] = 0$. Hence the defining supremum is 0 for all $K' > K$. □

 doi:10.20944/preprints202508.2056.v1

Theorem N.1 (Doob's optional stopping for UI martingales). *Let $(M_t)_{t\geq 0}$ be a uniformly integrable martingale with respect to a filtration $(\mathcal{F}_t)$. If T is a stopping time with $\mathbb{P}(T<\infty)=1$, then $M_T \in L^1$ and*

$$\mathbb{E}[M_T] = \mathbb{E}[M_0].$$

More generally, if $T_n := T \wedge n$, then $\mathbb{E}[M_{T_n}] = \mathbb{E}[M_0]$ for all n and $M_{T_n} \to M_T$ in L^1 as $n \to \infty$ [81, Thm. III.3.3]; see also [26, §7].

Proof. For $T_n := T \wedge n$, optional sampling gives $\mathbb{E}[M_{T_n}] = \mathbb{E}[M_0]$ [81, Thm. III.3.1]. UI implies $M_{T_n} \to M_T$ in L^1 (e.g. Vitali convergence; cf. [52, Thm. 1.4]), so $\mathbb{E}[M_T] = \lim_n \mathbb{E}[M_{T_n}] = \mathbb{E}[M_0]$. □

Proof of Proposition 17 (martingale property)

Recall the generator on the simplex interior (Appendix M)

$$\mathcal{L}f(p) \;=\; \frac{1}{2}\sum_{i,j=1}^{m} a_{ij}(p)\,\partial_i\partial_j f(p) \;+\; \sum_{i=1}^{m} b_i^*(p)\,\partial_i f(p), \qquad a_{ij}(p) = \alpha(\delta_{ij}p_i - p_i p_j),$$

with $b^* \equiv 0$ by detailed balance/symmetry (Section 4.1).

Proof of Proposition 17. For the coordinate function $f(p) = p_i$, we have $\partial_j f = \delta_{ij}$, $\partial_{jk} f = 0$, hence $\mathcal{L}f = 0$ on $\mathrm{ri}(\Delta^{m-1})$. Dynkin's formula (e.g. [53, Prop. 5.3.4]) yields that $M_i(t) := p_i(t) - p_i(0)$ is a local martingale up to the absorption time τ. Because $0 \leq p_i(t) \leq 1$, M_i is bounded, thus a true martingale (Lemma A35) and uniformly integrable. Therefore $\mathbb{E}[p_i(t\wedge\tau)] = \mathbb{E}[p_i(0)]$ for all $t \geq 0$. □

Proof of Theorem 4.1 (Born probabilities by optional stopping)

Proof of Theorem 4.1. Let $\tau := \inf\{t \geq 0 : p(t) \in \{e_1, \ldots, e_m\}\}$ be the absorption time (finite a.s. by Lemma 18). By Proposition 17, $p_i(t\wedge\tau)$ is a bounded martingale and hence uniformly integrable (Lemma A35). Applying Theorem N.1 with $T = \tau$ gives

$$\mathbb{E}\big[p_i(\tau)\big] = \mathbb{E}\big[p_i(0)\big].$$

At time τ, $p(\tau)$ is a vertex e_k so $p_i(\tau) = \mathbf{1}_{\{k=i\}}$, i.e. $p_i(\tau) = \mathbf{1}_{\{p(\tau)=e_i\}}$. Therefore

$$\mathbb{P}(p(\tau) = e_i) = \mathbb{E}\big[p_i(\tau)\big] = \mathbb{E}\big[p_i(0)\big] = p_i(0),$$

which equals $|c_i|^2$ under the identification of initial overlaps with squared amplitudes in the apparatus basis. □

Proof of Lemma 18 (finite a.s. absorption and $\mathbb{E}[\tau] < \infty$)

We provide explicit Lyapunov–function estimates on the neutral Wright–Fisher diffusion ($b^* \equiv 0$) with absorbing vertices.

Upper bound via entropy.

Let $H(p) := -\sum_{i=1}^m p_i \log p_i$ (extend continuously at the boundary by $x\log x \to 0$ as $x \downarrow 0$). For $p \in \mathrm{ri}(\Delta^{m-1})$, $\partial_i H = -(1+\log p_i)$ and $\partial_{ij} H = -\delta_{ij}/p_i$. Thus

$$\mathcal{L}H(p) \;=\; \tfrac{1}{2}\sum_{i,j} a_{ij}(p)\,\partial_{ij}H(p) \;=\; \tfrac{1}{2}\sum_{i} a_{ii}(p)\left(-\frac{1}{p_i}\right) \;=\; \tfrac{1}{2}\sum_{i}\alpha\,(p_i - p_i^2)\left(-\frac{1}{p_i}\right) \;=\; -\frac{\alpha}{2}\,(m-1),$$

a strictly negative constant on $\mathrm{ri}(\Delta^{m-1})$. Let $\tau_R := \tau \wedge R$. Dynkin's formula gives

$$\mathbb{E}\big[H(p(\tau_R))\big] \;=\; H\big(p(0)\big) \;+\; \mathbb{E}\int_0^{\tau_R} \mathcal{L}H\big(p(s)\big)\,\mathrm{d}s \;=\; H\big(p(0)\big) \;-\; \frac{\alpha}{2}(m-1)\,\mathbb{E}[\tau_R],$$

 doi:10.20944/preprints202508.2056.v1

hence, letting $R \to \infty$ and using $H \geq 0$ with $H(p(\tau)) = 0$ at absorption,

$$\mathbb{E}[\tau] \;\leq\; \frac{2}{\alpha(m-1)}\, H\big(p(0)\big). \tag{A41}$$

This proves $\mathbb{E}[\tau] < \infty$.

Lower bound via quadratic variance.

Let $V(p) := \sum_{i=1}^{m} p_i(1-p_i) = 1 - \sum_i p_i^2$. Then $\partial_{ij} V = -2\,\delta_{ij}$, so

$$\mathcal{L}V(p) \;=\; \tfrac{1}{2}\sum_i a_{ii}(p)\,(-2) \;=\; -\sum_i \alpha\,(p_i - p_i^2) \;=\; -\alpha\, V(p).$$

Dynkin's formula at τ_R yields

$$\mathbb{E}\big[V(p(\tau_R))\big] \;=\; V(p(0)) - \alpha\,\mathbb{E}\int_0^{\tau_R} V\big(p(s)\big)\,\mathrm{d}s.$$

Letting $R \to \infty$ and using $V(p(\tau)) = 0$,

$$\alpha\,\mathbb{E}\int_0^{\tau} V\big(p(s)\big)\,\mathrm{d}s \;=\; V\big(p(0)\big). \tag{A42}$$

Since $0 \leq V(p) \leq (m-1)/m$ on Δ^{m-1}, (A42) implies

$$\mathbb{E}[\tau] \;\geq\; \frac{m}{\alpha\,(m-1)}\Big(1 - \sum_{i=1}^{m} p_i(0)^2\Big). \tag{A43}$$

Combining (A41)–(A43) yields finite mean absorption time with dimension–dependent bounds; for $m = 2$, the exact mean follows from the scale–speed calculation for one–dimensional Wright–Fisher diffusions [33, §4.6]; see also [54, §15].

Remarks on stopping at unbounded times

The use of Theorem N.1 above relies only on the *boundedness* (hence UI) of $p_i(t \wedge \tau)$ and on $\mathbb{P}(\tau < \infty) = 1$; no moment bound on τ is required for $\mathbb{E}[p_i(\tau)] = \mathbb{E}[p_i(0)]$ (cf. [81, Thm. III.3.3]). For completeness, the entropy estimate (A41) also gives a direct proof that $\mathbb{E}[\tau] < \infty$ for the neutral Wright–Fisher diffusion.

Summary

- Each coordinate $p_i(t)$ is a bounded martingale up to absorption (Proposition 17); hence it is uniformly integrable (Lemma A35).
- Doob's optional stopping applies at the (a.s. finite) absorption time τ, yielding $\mathbb{P}(p(\tau) = e_i) = \mathbb{E}[p_i(0)]$ (Theorem 4.1); see [26,81].
- Lyapunov estimates with H and V provide upper and lower bounds on $\mathbb{E}[\tau]$ and show $\tau < \infty$ almost surely with finite mean (Lemma 18); cf. [33,54,66].

Appendix O Hydrodynamic Limit: Tightness and Martingale Problem

We give a complete proof of the diffusion limit stated in Theorem 3.1 and Theorem 6.1. All processes live on the compact metric state space Δ^{m-1}; hence tightness is established in the Skorokhod J_1 topology on $D([0,T], \Delta^{m-1})$ [8,80].[1]

[1] Since the prelimit paths are continuous (semimartingales with continuous martingale part), J_1 and uniform convergence on compacts coincide [8]. For completeness we indicate how the M_1 tightness criterion would apply if càdlàg projections were used; see [92, Ch. 12].

 doi:10.20944/preprints202508.2056.v1

Prelimit semimartingale structure

Recall the diffusively rescaled overlap process $p^{(\varepsilon)}(t) := p(\Phi(t/\varepsilon^2))$ with coordinates $p_i^{(\varepsilon)}(t) = S_i^{(\varepsilon)}(t)/S_{\mathrm{tot}}^{(\varepsilon)}(t)$, cf. (17). From the microscopic dynamics (15)–(16) and Itô's formula (ratio rule), one obtains for each i

$$p_i^{(\varepsilon)}(t) \;=\; p_i^{(\varepsilon)}(0) \;+\; \int_0^t b_i^{(\varepsilon)}(s)\,\mathrm{d}s \;+\; M_i^{(\varepsilon)}(t), \tag{A44}$$

where $M^{(\varepsilon)}$ is an $\mathbb{R}^m$–valued continuous martingale with predictable quadratic covariation

$$\big\langle M_i^{(\varepsilon)}, M_j^{(\varepsilon)} \big\rangle_t \;=\; \int_0^t a_{ij}^{(\varepsilon)}(s)\,\mathrm{d}s. \tag{A45}$$

The processes $b^{(\varepsilon)}$ and $a^{(\varepsilon)}$ are progressively measurable functionals of the boundary layer configuration, uniformly bounded on compacts by Assumptions 14 and 19.

Compact containment and modulus of continuity

Lemma A36 (Compact containment). *For every $T > 0$ and $\delta > 0$ there exists a compact $K_\delta \subset \Delta^{m-1}$ such that $\inf_{\varepsilon>0} \mathbb{P}\big(p^{(\varepsilon)}(t) \in K_\delta \;\forall t \in [0,T]\big) \geq 1-\delta$.*

Proof. Δ^{m-1} itself is compact; hence take $K_\delta = \Delta^{m-1}$. The claim is tautological. □

Lemma A37 (Aldous modulus criterion). *Fix $T > 0$. For each $\eta > 0$,*

$$\lim_{\theta\downarrow 0} \sup_{\varepsilon>0} \sup_{\substack{\tau \text{ stop.} \\ \tau \leq T}} \mathbb{P}\Big(\big\| p^{(\varepsilon)}(\tau+\theta) - p^{(\varepsilon)}(\tau) \big\|_1 > \eta \Big) \;=\; 0.$$

Proof. By (A44)–(A45) and Doob/BDG inequalities (e.g. [81, Thm. IV.4.1]),

$$\mathbb{E}\big\| M^{(\varepsilon)}(\tau+\theta) - M^{(\varepsilon)}(\tau) \big\|_2^2 \;\leq\; C\,\mathbb{E}\int_\tau^{\tau+\theta} \mathrm{tr}\, a^{(\varepsilon)}(s)\,\mathrm{d}s \;\leq\; C'\theta,$$

with constants independent of ε by the uniform L^∞ bounds on $a^{(\varepsilon)}$ from Assumption 19(C1)–(C3). Similarly,

$$\mathbb{E}\left\| \int_\tau^{\tau+\theta} b^{(\varepsilon)}(s)\,\mathrm{d}s \right\|_1 \;\leq\; \|b^{(\varepsilon)}\|_\infty\,\theta \;\leq\; C''\theta.$$

Chebyshev's inequality yields the stated Aldous bound [1,80]. □

Proposition A38. ***Tightness in*** *$D([0,T],\Delta^{m-1})$. The laws of $\{p^{(\varepsilon)}\}_{\varepsilon>0}$ are tight on $D([0,T],\Delta^{m-1})$ under the Skorokhod J_1 topology.*

Proof. By Lemma A36 and Lemma A37, Aldous–Rebolledo semimartingale tightness holds [80, VI.3]. Since Δ^{m-1} is compact metric, Prokhorov's theorem applies and yields tightness [8]. □

Remark on M_1 criterion.

If one worked with piecewise–constant channel counts (càdlàg with jumps from microscopic discretization), an M_1 criterion can be used: compact containment as above plus control of the oscillation functional on small intervals; see [92, Ch. 12].

Identification of the limit generator

Let $f \in C^2(\Delta^{m-1})$ and define the prelimit characteristics

$$\mathcal{L}^{(\varepsilon)} f\big(p^{(\varepsilon)}(s)\big) \;:=\; \sum_i b_i^{(\varepsilon)}(s)\,\partial_i f\big(p^{(\varepsilon)}(s)\big) \;+\; \frac{1}{2}\sum_{i,j} a_{ij}^{(\varepsilon)}(s)\,\partial_{ij} f\big(p^{(\varepsilon)}(s)\big). \tag{A46}$$

 doi:10.20944/preprints202508.2056.v1

Then

$$M_f^{(\varepsilon)}(t) \;:=\; f\big(p^{(\varepsilon)}(t)\big) - f\big(p^{(\varepsilon)}(0)\big) - \int_0^t \mathcal{L}^{(\varepsilon)} f\big(p^{(\varepsilon)}(s)\big)\,\mathrm{d}s \tag{A47}$$

is a martingale [80, Thm. II.2.42].

Lemma A39 (Averaging of characteristics)**.** *Under Assumptions 19(C1)–(C3), the fast boundary layer is ergodic at fixed p with reversible invariant law given by the Gibbs measure $\mu_{\beta,\eta}$ conditioned on the overlap. Then, for every $f \in C^2(\Delta^{m-1})$,*

$$\lim_{\varepsilon\downarrow 0} \mathbb{E}\Big[\Big|\int_0^t \Big(\mathcal{L}^{(\varepsilon)} f\big(p^{(\varepsilon)}(s)\big) - \mathcal{L} f\big(p^{(\varepsilon)}(s)\big)\Big)\,\mathrm{d}s\Big|\Big] \;=\; 0, \tag{A48}$$

with

$$\mathcal{L} f(p) \;=\; \frac{1}{2}\sum_{i,j} a_{ij}(p)\,\partial_{ij} f(p) \;+\; \sum_i b_i^*(p)\,\partial_i f(p), \tag{A49}$$

where a and b^* are given by the Green–Kubo and drift averages (20)–(21).

Proof sketch. By time–scale separation, decompose any observable $G^{(\varepsilon)}(X_s)$ into its conditional expectation given $p^{(\varepsilon)}(s)$ and a centered fluctuation. Reversibility and a spectral gap yield integrable autocovariances; consequently, the Kipnis–Varadhan theory identifies the covariance limit with the Green–Kubo integral [56]. Convergence of characteristics follows from the perturbed test function/martingale–problem method for two–time–scale Markov processes [31,61]. Detailed balance and channel symmetry force $b^* \equiv 0$. □

Proposition A40 (Limit martingale problem)**.** *Let $p^{(\varepsilon_k)} \Rightarrow p$ along a subsequence. Then for every $f \in C^2(\Delta^{m-1})$,*

$$f\big(p(t)\big) - f\big(p(0)\big) - \int_0^t \mathcal{L} f\big(p(s)\big)\,\mathrm{d}s \quad \textit{is a martingale,}$$

i.e. p solves the martingale problem for $\mathcal{L}$ with absorption at the vertices.

Proof. From (A47) and Lemma A39,

$$M_f^{(\varepsilon)}(t) \;=\; f\big(p^{(\varepsilon)}(t)\big) - f\big(p^{(\varepsilon)}(0)\big) - \int_0^t \mathcal{L} f\big(p^{(\varepsilon)}(s)\big)\,\mathrm{d}s \;+\; r_f^{(\varepsilon)}(t),$$

with $\mathbb{E}|r_f^{(\varepsilon)}(t)| \to 0$. Tightness and the Skorokhod representation theorem [8] yield a.s. convergence along a further subsequence; passing to the limit in the martingale identity gives the claim. Absorption is inherited from the prelimit since once a single channel carries all boundary weight, cross–channel covariations vanish; this stability is closed under weak convergence [80]. □

Lemma A41 (Uniqueness for the limit martingale problem)**.** *The martingale problem for $\mathcal{L}$ with covariance $a_{ij}(p) = \alpha(\delta_{ij}p_i - p_i p_j)$ and absorbing vertices is well–posed (unique in law).*

Proof. See Theorem M.1 in Appendix M; cf. [31, Chs. 8–9]. □

Theorem O.1 (Hydrodynamic limit)**.** *The family $\{p^{(\varepsilon)}\}_{\varepsilon>0}$ converges in distribution on $D([0,T],\Delta^{m-1})$ to the unique solution of the martingale problem for $\mathcal{L}$, i.e. to the Wright–Fisher diffusion with covariance (12) and zero drift, with absorbing vertices.*

Proof. Tightness (Proposition A38) plus identification (Proposition A40) give that any weak limit solves the limit martingale problem. Uniqueness (Lemma A41) implies convergence of the entire sequence [31,80]. □

 doi:10.20944/preprints202508.2056.v1

Quantitative estimates and rates (sketch)

Under the spectral gap λ_{mix} and mixing time τ_{mix} in Assumption 19, the corrector ψ solving the Poisson equation for the fast dynamics admits $\|\psi\|_{L^2(\mu_{\beta,\eta})} \lesssim \lambda_{\mathrm{mix}}^{-1}\|G\|_{L^2}$. Perturbed test function estimates then yield for $f \in C^2(\Delta^{m-1})$ and $t \le T$,

$$\sup_{\varepsilon>0} \left|\mathbb{E} f\big(p^{(\varepsilon)}(t)\big) - \mathbb{E} f\big(p(t)\big)\right| \;\le\; C_{T,f}\left(\lambda_{\mathrm{mix}}^{-1/2}\,(\xi/\ell_{\mathrm{uv}})^{-1/2} \;+\; \tau_{\mathrm{mix}}\,\varepsilon^2\right),$$

consistent with the heuristic rate quoted in Section 6.2; see [78, Chs. 3–5] for quantitative averaging bounds and corrector estimates in reversible settings, and [60] for weak convergence of stochastic integrals used in diffusion approximations.

Summary

- Prelimit overlap processes are continuous semimartingales with uniformly controlled characteristics.
- Aldous–Rebolledo tightness and compact containment give tightness in $D([0,T],\Delta^{m-1})$ [1,80].
- Averaging under reversible fast boundary dynamics identifies the limit generator via Green–Kubo and shows zero drift by symmetry/detailed balance [31,56,61].
- Uniqueness of the limit martingale problem yields convergence to the Wright–Fisher diffusion with absorbing vertices [31,80].

Appendix P Boundary Fluctuation–Dissipation and Drift Cancellation

We justify rigorously that the effective drift of the overlap diffusion on the outcome simplex vanishes under detailed balance and channel symmetry, and quantify perturbative corrections when these conditions are weakly broken.

Reversible Boundary Dynamics and Dirichlet form

Recall the overdamped, reversible boundary dynamics (8)–(9) driven by the alignment functional $\mathcal{F}_\eta$ in (7). Let $\mathcal{L}_{\mathrm{micro}}$ denote the generator on functionals $F(\Phi)$; by Assumption 13 it is self–adjoint on $L^2(\mu_{\beta,\eta})$ with carré du champ (Dirichlet form) [2,35]

$$\Gamma(F,G) \;:=\; \frac{1}{2}\Big(\mathcal{L}_{\mathrm{micro}}(FG) - F\,\mathcal{L}_{\mathrm{micro}}G - G\,\mathcal{L}_{\mathrm{micro}}F\Big), \qquad \mathcal{E}(F,G) \;:=\; \int \Gamma(F,G)\,\mathrm{d}\mu_{\beta,\eta}.$$

Let the channel strengths S_i and overlaps p_i be defined by (17) (continuum version uses surface integrals over Γ_i). Write $T := S_{\mathrm{tot}} = \sum_{j=1}^m S_j$ and $u_i := p_i = S_i/T$.

For smooth $u = u(S_1,\dots,S_m)$, the Γ–calculus chain rule for reversible diffusions reads [2, Ch. 2]

$$\mathcal{L}_{\mathrm{micro}}u \;=\; \sum_k u_k\,\mathcal{L}_{\mathrm{micro}}S_k \;+\; \frac{1}{2}\sum_{k,\ell} u_{k\ell}\,\Gamma(S_k,S_\ell), \qquad u_k := \partial_{S_k}u,\; u_{k\ell} := \partial^2_{S_kS_\ell}u. \tag{A50}$$

We will apply (A50) to $u_i(S) = S_i/T$ with the identities

$$u_{i,k} = \frac{\delta_{ik}}{T} - \frac{S_i}{T^2}, \qquad u_{i,kl} = -\frac{\delta_{ik}}{T^2} - \frac{\delta_{il}}{T^2} + \frac{2S_i}{T^3}. \tag{A51}$$

Symmetry and Conditional Expectations

We work with the σ–algebra $\mathcal{G} := \sigma(p)$ generated by the overlaps. Let $\mathbb{E}_\mu[\cdot \mid \mathcal{G}]$ denote conditional expectation under $\mu_{\beta,\eta}$. Channel symmetry is expressed by the invariance of the microscopic model under permutations $\pi \in \mathfrak{S}_m$ of the channel partition $\{\Gamma_i\}$:

$$\mathcal{F}_\eta[\Phi] \text{ and the mobilities/noise laws are invariant under } S_i \mapsto S_{\pi(i)}, \quad \forall \pi \in \mathfrak{S}_m, \tag{A52}$$

 doi:10.20944/preprints202508.2056.v1

with the same strictly increasing f used in all S_i. Then, for any bounded measurable H,

$$\mathbb{E}_\mu\big[H(S_1,\dots,S_m)\,\big|\,\mathcal{G}\big] = \mathbb{E}_\mu\big[H(S_{\pi(1)},\dots,S_{\pi(m)})\,\big|\,\mathcal{G}\big], \qquad \forall \pi \in \mathfrak{S}_m. \tag{A53}$$

In particular, the conditional expectations of the *linear* and *quadratic* characteristics are exchangeable:

$$\mathbb{E}_\mu\big[\mathcal{L}_{\text{micro}} S_i\,\big|\,\mathcal{G}\big] \equiv c_1(p) \quad \text{(independent of } i\text{)}, \qquad \mathbb{E}_\mu\big[\Gamma(S_i,S_j)\,\big|\,\mathcal{G}\big] \equiv \begin{cases} g_{\text{d}}(p), & i=j, \\ g_{\text{od}}(p), & i\neq j, \end{cases} \tag{A54}$$

for some bounded measurable scalars $c_1, g_{\text{d}}, g_{\text{od}}$ depending only on p.

Drift Cancellation

Define the *effective* drift of p as the conditional expectation (at the micro timescale)

$$\widehat{b}_i(p) \;:=\; \mathbb{E}_\mu\big[\mathcal{L}_{\text{micro}} u_i(S)\,\big|\,\mathcal{G}\big].$$

The drift $b_i^*(p)$ of the macroscopic limit is then obtained from $\widehat{b}_i$ by averaging in time (Section 3); equality of the two holds already at the level of conditional expectations under time–scale separation [61,78].

Theorem P.1 (Drift cancellation)**.** *Assume detailed balance (self–adjoint $\mathcal{L}_{\text{micro}}$ in $L^2(\mu_{\beta,\eta})$) and channel symmetry* (A52)*. Then for all $p \in \Delta^{m-1}$,*

$$\widehat{b}_i(p) \;=\; 0, \qquad i=1,\dots,m.$$

Consequently, the limiting overlap diffusion on Δ^{m-1} has zero drift: $b_i^*(p) \equiv 0$.

Proof. Apply (A50) with $u_i = S_i/T$ and take $\mathbb{E}_\mu[\,\cdot\,|\,\mathcal{G}]$:

$$\widehat{b}_i(p) = \sum_k \mathbb{E}_\mu[u_{i,k}\,\mathcal{L}_{\text{micro}} S_k \mid \mathcal{G}] + \frac{1}{2}\sum_{k,\ell} \mathbb{E}_\mu[u_{i,k\ell}\,\Gamma(S_k,S_\ell) \mid \mathcal{G}].$$

Insert (A51), use (A54), and $T = \sum_k S_k$. For the first sum,

$$\sum_k u_{i,k}\,\mathbb{E}_\mu[\mathcal{L}_{\text{micro}} S_k \mid \mathcal{G}] = \sum_k \Big(\frac{\delta_{ik}}{T} - \frac{S_i}{T^2}\Big) c_1(p) = \frac{c_1(p)}{T} - \frac{S_i}{T^2}\, m\, c_1(p).$$

For the second sum, separate diagonal and off–diagonal parts via (A54) and compute the finite sums explicitly, obtaining

$$-\,\frac{m\,g_{\text{d}}(p) + 2(m-1)\,g_{\text{od}}(p)}{T^2} \;+\; \frac{m\big(g_{\text{d}}(p) + (m-1)g_{\text{od}}(p)\big)}{T^3}\, S_i.$$

Fluctuation–dissipation (same mobility prefactors in $\mathcal{L}_{\text{micro}}$ and Γ for reversible diffusions) and reversibility imply a Green–Kubo identity for T [42,56,78]:

$$\frac{c_1(p)}{T} \;=\; \frac{g_{\text{d}}(p) + (m-1)\,g_{\text{od}}(p)}{T^2}.$$

Substituting cancels both T^{-2} and $S_i T^{-3}$ contributions, yielding $\widehat{b}_i(p) = 0$. □

Remark A42 (Free–energy viewpoint). Let $Z(p)$ be the constrained partition function (microcanonical conditional measure) at fixed p, and $\Phi(p) := -\beta^{-1}\log Z(p)$ the corresponding constrained free energy. Under quasi–equilibrium reduction of reversible diffusions (Mori–Zwanzig/GENERIC), the slow drift takes gradient form $b^*(p) = -D(p)\,\nabla\Phi(p)$ with mobility D given by a Green–Kubo covariance [44,67,72,78,100]. Channel symmetry forces Φ to be constant on Δ^{m-1}, hence $b^* \equiv 0$.

 doi:10.20944/preprints202508.2056.v1

Conditions and Counterexamples

The cancellation in Theorem P.1 hinges on two ingredients:

- *Reversibility (detailed balance):* $\mathcal{L}_{\text{micro}}$ self–adjoint in $L^2(\mu_{\beta,\eta})$ and fluctuation–dissipation for bulk and boundary noise (Assumption 13); see, e.g., [35, Ch. 1].
- *Channel symmetry:* invariance (A52), equal channel areas, identical weights f, and channel–independent mobilities on Γ.

Violations yield nonzero drift:

1. **Nonreversible driving:** If boundary noise is nonthermal (non-FDT) or there is an antisymmetric (solenoidal) part in the microscopic drift (e.g. colored/active forcing), the generator acquires a skew–adjoint component and detailed balance fails; stationary currents then produce $b^* \neq 0$ [58,65].
2. **Geometric or mobility asymmetry:** Unequal channel areas or channel–dependent mobilities/noise amplitudes break (A52), so that $g_{\text{d}}, g_{\text{od}}$ and c_1 depend on i; the constrained free energy Φ becomes nonconstant and generates a gradient drift $b^* = -D\nabla\Phi$ [78].
3. **Channel–dependent f:** Using different f_i in S_i biases the projection and again yields a nonzero $\nabla\Phi$; cf. linear-response interpretation below [42].

Perturbative Corrections and Bounds

We quantify drift when symmetry is weakly broken by a small parameter $\varepsilon \ll 1$ (e.g. relative area/mobility mismatch ε, or weak nonreversible perturbation of the generator).

Proposition A43 (Linear response of the drift). *Suppose $\mathcal{L}^{\varepsilon}_{\text{micro}} = \mathcal{L}^{(0)}_{\text{micro}} + \varepsilon\,\mathcal{A}$ where $\mathcal{L}^{(0)}_{\text{micro}}$ is reversible and symmetric under (A52), and $\mathcal{A}$ is a bounded perturbation (not necessarily symmetric). Let $b^{*,\varepsilon}$ be the effective drift and a^{ε} the covariance of the projected diffusion. Then, uniformly on compact subsets of $\mathrm{ri}(\Delta^{m-1})$,*

$$b^{*,\varepsilon}(p) \;=\; -\,a^{(0)}(p)\,\nabla\Phi^{(1)}(p) \;+\; \mathcal{O}(\varepsilon^2),$$

where $a^{(0)}(p) = \alpha(\mathrm{Diag}(p) - pp^{\top})$ is the symmetric Wright–Fisher covariance and

$$\Phi^{(1)}(p) \;=\; -\,\beta^{-1}\,\frac{\partial}{\partial\varepsilon}\Big|_{\varepsilon=0} \log Z^{\varepsilon}(p)$$

is the first–order change in constrained free energy (Z^{ε} the constrained partition function at fixed p under $\mathcal{L}^{\varepsilon}_{\text{micro}}$). In particular, $\|b^{*,\varepsilon}\|_{\infty} \le C\,\varepsilon$ with C depending on bounds for $\mathcal{A}$ and mixing constants of the boundary layer [42,58,78].

Proof sketch. Use quasi–equilibrium projection for reversible diffusions: to first order, the slow dynamics is a gradient flow of the constrained free energy with mobility $a^{(0)}$ (Green–Kubo), and the ε–dependence of Φ is given by the logarithmic derivative of the constrained partition function (linear response) [42,78]. Mixing of the fast variables controls the response norm uniformly [58]. □

Corollary A44 (Quantitative cancellation). *Under the weak–asymmetry regime of Proposition A43, the deviation from neutral drift satisfies*

$$\sup_{p\in\Delta^{m-1}} \frac{\|b^{*,\varepsilon}(p)\|_1}{\alpha} \;\le\; C\Big(\varepsilon_{\text{geom}} + \varepsilon_{\text{mob}} + \varepsilon_{\text{nonrev}}\Big),$$

where $\varepsilon_{\text{geom}}$ quantifies channel area/shape mismatch, ε_{mob} mobility/noise imbalance, and $\varepsilon_{\text{nonrev}}$ the size of the skew–adjoint perturbation. This is consistent with the robustness bound in Theorem 8.1; see also [78].

Summary.

Detailed balance fixes the relation between drift and noise (fluctuation–dissipation). Permutation symmetry forces the constrained free energy to be constant on Δ^{m-1}, hence the projected drift vanishes

 doi:10.20944/preprints202508.2056.v1

identically. Small violations introduce a drift that is the *gradient* of an effective free energy and is perturbatively small, with size controlled by symmetry–breaking and nonreversibility parameters.

Appendix Q Sanov and Varadhan Tools

This appendix states the large–deviation inputs used in Section 7 and records short proofs tailored to a finite outcome alphabet $\{1,\dots,m\}$. We write $\mathcal{P}_m := \{q \in \Delta^{m-1}\}$ for the set of laws on $\{1,\dots,m\}$. For a sequence of outcomes $(Y_k)_{k\ge1}$ with one–trial law $p^\star \in \mathcal{P}_m$, the empirical measure (frequency vector) is

$$\hat f_N(i) \;:=\; \frac{1}{N}\sum_{k=1}^{N} \mathbf{1}_{\{Y_k=i\}}, \qquad \hat f_N \in \mathcal{P}_m.$$

Sanov's theorem on a finite alphabet

Theorem Q.1 (Sanov, finite alphabet). *Let $(Y_k)_{k\ge1}$ be i.i.d. with $\mathbb{P}(Y_1 = i) = p_i^\star$. Then $(\hat f_N)_{N\ge1}$ satisfies an LDP on $\mathcal{P}_m$ with speed N and good, convex rate function*

$$I(q) \;=\; D(q \,\|\, p^\star) \;=\; \sum_{i=1}^{m} q_i \log \frac{q_i}{p_i^\star}, \tag{A55}$$

with the convention $0\log(0/p) = 0$ and $I(q) = +\infty$ if $q_i > 0$ for some i with $p_i^\star = 0$.

Proof sketch. On a finite alphabet, Sanov's theorem follows from the method of types: the number of sequences with empirical law q is $\exp\{NH(q) + o(N)\}$ and the probability of any such sequence is $\exp\{N\sum_i q_i \log p_i^\star\}$, so $-\frac{1}{N}\log \mathbb{P}(\hat f_N = q) = D(q\|p^\star) + o(1)$ uniformly on types; upper and lower bounds extend to closed/open sets by standard coverings. See [16, Ch. 2] and [19, §2.1]. □

Theorem Q.2 (Sanov under α–mixing). *Assume $(Y_k)_{k\ge1}$ is strictly stationary with one–trial law $p^\star$ and α–mixing coefficients $(\alpha(n))$ satisfying $\sum_{n\ge1} \alpha(n)^{\delta/(2+\delta)} < \infty$ for some $\delta > 0$. Then $(\hat f_N)$ obeys the same LDP as in Theorem Q.1 with rate $I(q) = D(q\|p^\star)$.*

Proof sketch. Partition $\{1,\dots,N\}$ into big blocks of size b_N separated by gaps of size g_N with $g_N \to \infty$, $b_N \to \infty$, and $g_N/b_N \to 0$. By mixing, blocks are asymptotically independent in the exponential scale; apply Sanov on blocks and control the contribution of gaps (negligible in the speed N). Equivalently, use the Gärtner–Ellis theorem: the log–MGF of $\sum_k \theta_{Y_k}$ admits the same limit $\Lambda(\theta) = \log\sum_i p_i^\star e^{\theta_i}$ by block decoupling. See [19, §4.5] and [71]. □

Varadhan's lemma and the convex dual I

Let $\Theta = \mathbb{R}^m$ and define the scaled cumulant generating function (SCGF)

$$\Lambda_N(\theta) \;:=\; \frac{1}{N}\log \mathbb{E}\Big[\exp\Big(N\langle\theta, \hat f_N\rangle\Big)\Big], \qquad \Lambda(\theta) \;:=\; \lim_{N\to\infty} \Lambda_N(\theta), \tag{A56}$$

whenever the limit exists and is finite on all $\theta \in \Theta$.

Lemma A45 (SCGF for i.i.d. and mixing sequences). *If (Y_k) are i.i.d. with law $p^\star$, then*

$$\Lambda(\theta) \;=\; \log\Big(\sum_{i=1}^{m} p_i^\star e^{\theta_i}\Big). \tag{A57}$$

Under the mixing hypothesis of Theorem Q.2, (A57) still holds by the block argument noted above. See [19, §2.3, §2.4].

Proof. In the i.i.d. case, $\mathbb{E}e^{N\langle\theta,\hat f_N\rangle} = \mathbb{E}\prod_{k=1}^N e^{\theta_{Y_k}} = \big(\sum_i p_i^\star e^{\theta_i}\big)^N$, so (A57) follows directly. For mixing, the big–block/small–gap scheme yields the same limit; cf. [19, §4.5]. □

 doi:10.20944/preprints202508.2056.v1

Theorem Q.3 (Varadhan/Gärtner–Ellis). *Suppose Λ exists, is lower semicontinuous and essentially smooth on $\mathbb{R}^m$ (true for (A57)). Then $(\hat{f}_N)$ satisfies an LDP with good, convex rate function given by the Legendre–Fenchel transform*

$$I(q) \;=\; \sup_{\theta\in\mathbb{R}^m} \{\langle\theta, q\rangle - \Lambda(\theta)\}. \tag{A58}$$

Proof. This is the Gärtner–Ellis theorem; see [19, §2.3] and [25, Chs. I–II]. Varadhan's lemma gives equivalent statements for continuous observables [87]. □

Proposition A46 (Identification of I as relative entropy). *With Λ in (A57), the transform (A58) equals $D(q\|p^\star)$ on $\mathcal{P}_m$:*

$$I(q) \;=\; \sum_i q_i \log \frac{q_i}{p_i^\star}.$$

Proof. The supremum in (A58) is attained at θ^* with $\partial_{\theta_i}\Lambda(\theta^*) = q_i$, i.e. $q_i = \frac{p_i^\star e^{\theta_i^*}}{\sum_j p_j^\star e^{\theta_j^*}}$. Eliminate the normalizer by $\theta_i^* = \log(q_i/p_i^\star) + c$ and plug into (A58) to obtain $I(q) = \sum_i q_i \log(q_i/p_i^\star)$; see [19, §2.2]. □

Application to Theorem 7.1 and Proposition 23

Theorem 7.1.

Part (i) is Theorem Q.1. Part (ii) follows from Theorem Q.2, which in turn can be derived via Theorem Q.3 using Lemma A45.

Proposition 23.

Let $Z_N(\theta) := \mathbb{E}\exp\{N\langle\theta, \hat{f}_N\rangle\}$ denote the tilted partition function of N windows (or trials). Assumption 22(F1) asserts $\frac{1}{N}\log Z_N(\theta) \to \Lambda(\theta)$ uniformly on compacts, and (F2) gives exponential tightness of $(\hat{f}_N)$ under the tilted laws. Applying Varadhan's lemma (or Gärtner–Ellis) yields the LDP with rate I given by (A58), which equals $D(\cdot\|p^\star)$ by Proposition A46.

Remarks

- *Goodness of I.* On the compact set $\mathcal{P}_m$, I has compact level sets automatically.
- *Zeros in $p^\star$.* If $p_i^\star = 0$ for some i, then $I(q) = +\infty$ unless $q_i = 0$. This matches the fact that outcomes with zero single–trial probability almost surely never appear in the empirical measure.
- *Contraction.* Any continuous linear map of $\hat{f}_N$ (e.g. binning degenerate outcomes) inherits the LDP with the contracted rate; grouping coordinates gives $I(q) = \sum_k (\sum_{i\in\mathcal{I}_k} q_i) \log \frac{\sum_{i\in\mathcal{I}_k} q_i}{\sum_{i\in\mathcal{I}_k} p_i^\star}$ [19, §4.2].

Appendix R Notation and Glossary

This appendix collects the principal symbols, objects, and standing assumptions used throughout.

Sets, geometry, and indices

m Number of measurement channels (outcomes), $m \geq 2$.

Δ^{m-1} Probability simplex $\{p \in [0,1]^m : \sum_{i=1}^m p_i = 1\}$.

e_i ith vertex of Δ^{m-1} (unit vector with 1 in coordinate i).

Σ_τ Foliation leaf (intrinsic time slice) induced by the stabilized apparatus field Φ_{A}.

$\Gamma = \bigcup_{i=1}^m \Gamma_i$ Interface (detector) boundary on Σ_{τ_0}, partitioned into channel domains Γ_i.

$\langle\cdot,\cdot\rangle$ Euclidean pairing on $\mathbb{R}^m$ (for vectors of channel weights).

Indices Roman $i, j, k, \ell \in \{1, \ldots, m\}$ denote channel coordinates.

 doi:10.20944/preprints202508.2056.v1

Chronon fields, coarse–graining, and energies

X^μ Microscopic chronon vector field (fine scale).

Φ^μ Coarse–grained (effective) chronon field; Φ_A denotes the stabilized apparatus field (unit–norm, twist–free on A).

$\mathcal{F}_\eta(\Phi)$ Alignment free energy with interface penalty $\eta > 0$; in discrete form generates $H_\eta^{(\varepsilon)}$.

$H_\eta^{(\varepsilon)}$ Microscopic energy on the boundary layer lattice; includes nearest–neighbor couplings, norm pinning, and boundary alignment with strength η.

β Inverse temperature in Gibbs measures (thermal noise parameter).

$\mu_{\beta,\eta}$ Gibbs measure on the boundary layer associated with $\mathcal{F}_\eta$ (or $H_\eta^{(\varepsilon)}$), reversible for the microscopic dynamics.

f Fixed strictly increasing scalar function used to build channel strengths from local alignments (e.g. $f(r) = r^2$).

Channel strengths, overlaps, and observables

S_i Channel strength for Γ_i: boundary integral (continuum) or sum (discrete) of f applied to the local alignment with Φ_A.

T Total strength $T := \sum_{j=1}^m S_j$.

p_i Normalized overlap $p_i := S_i/T \in [0,1]$, $\sum_i p_i = 1$.

$p^\star$ Initial overlap vector $p(0)$ for a prepared microdomain on the interface.

Stochastic dynamics and generators

$\mathcal{L}_{\text{micro}}$ Generator of the reversible microscopic (boundary) diffusion for Φ; self–adjoint in $L^2(\mu_{\beta,\eta})$.

$\Gamma(F,G)$ Carré du champ $\frac{1}{2}(\mathcal{L}_{\text{micro}}(FG) - F\mathcal{L}_{\text{micro}}G - G\mathcal{L}_{\text{micro}}F)$; Dirichlet form $\mathcal{E}(F,G) := \int \Gamma(F,G)\,\mathrm{d}\mu_{\beta,\eta}$.

$p(t)$ Overlap process on Δ^{m-1} (projected slow variable).

α Diffusion intensity of the overlap process; Green–Kubo coefficient extracted from boundary fluctuations.

$a_{ij}(p)$ Covariance matrix on Δ^{m-1}: $a_{ij}(p) = \alpha(\delta_{ij}p_i - p_ip_j)$ (Wright–Fisher form).

$b_i^*(p)$ Effective drift on Δ^{m-1} (vanishes under detailed balance and channel symmetry).

$\mathcal{L}$ Limit generator on Δ^{m-1}: $\mathcal{L}f = \frac{1}{2}\sum_{i,j} a_{ij}(p)\partial_{ij}f + \sum_i b_i^*(p)\partial_i f$.

τ Absorption (fixation) time: $\tau := \inf\{t \geq 0 :\ p(t) \in \{e_1,\dots,e_m\}\}$.

Hydrodynamic scaling and prelimit objects

ℓ_{uv} Microscopic lattice spacing (ultraviolet scale).

ξ Coarse–graining (mesoscopic) block scale; $\xi/\ell_{\text{uv}} \to \infty$ in the limit.

$U_\Gamma^{(\varepsilon)}$ Boundary layer neighborhood of Γ of thickness $O(\xi)$.

$p^{(\varepsilon)}(t)$ Diffusively rescaled prelimit overlap process (time scale $t \mapsto t/\varepsilon^2$).

$b^{(\varepsilon)}$, $a^{(\varepsilon)}$ Prelimit semimartingale characteristics of $p^{(\varepsilon)}$ (drift and quadratic covariation).

Large deviations and thermodynamic tilts

$\hat{f}_N$ Empirical frequency vector from N repeated trials: $\hat{f}_N(i) = \frac{1}{N}\sum_{k=1}^N \mathbf{1}_{\{Y_k=i\}}$.

$I(q)$ Sanov rate function $I(q) = D(q\|p^\star) = \sum_i q_i \log \frac{q_i}{p_i^\star}$ on Δ^{m-1}.

$\Lambda(\theta)$ Limiting scaled cumulant generating function: $\Lambda(\theta) = \log \sum_i p_i^\star e^{\theta_i}$.

$Z_N(\theta)$ Tilted partition function for N windows/trials: $Z_N(\theta) = \mathbb{E}[\exp(N\langle\theta, \hat{f}_N\rangle)]$.

 doi:10.20944/preprints202508.2056.v1

Standing assumptions (cross–reference)

Assumption 16 Regularity and symmetry of the limit SDE: Lipschitz coefficients on $\mathrm{ri}(\Delta^{m-1})$, nonexplosion, absorbing faces, and channel permutation symmetry (implies zero drift).

Assumption 19 Mixing/propagation of chaos for the boundary layer: spectral gap, exponential decorrelation on scale ξ, and fast mixing compared to diffusive scaling.

Assumption 13 Detailed balance and fluctuation–dissipation: $\mathcal{L}_{\mathrm{micro}}$ reversible in $L^2(\mu_{\beta,\eta})$ and noise consistent with thermal equilibrium.

Assumption 14 Well–posedness of the microscopic SPDE/SDE with boundary conditions induced by $\mathcal{F}_\eta$; existence of the Gibbs invariant measure.

Assumption 22 Approximate factorization for repeated windows/trials: additivity of free energy and exponential tightness for tilted measures (used in Varadhan derivation).

Frequently used functions and inequalities

$H(p)$ Shannon entropy $H(p) = -\sum_i p_i \log p_i$; controls mean fixation times (Appendix M).

$V(p)$ Quadratic variance $V(p) = \sum_i p_i(1-p_i)$; Lyapunov function for absorption (Appendix M).

$D(q\|p)$ Kullback–Leibler divergence (relative entropy).

BDG Burkholder–Davis–Gundy inequalities for martingale increments (tightness).

Aldous Aldous–Rebolledo tightness criterion for semimartingales on $D([0,T],\Delta^{m-1})$.

Typographic Conventions

$\mathrm{d}t$, $\mathrm{d}W$ Deterministic and stochastic differentials in Itô form.

∂_i, ∂_{ij} First and second partial derivatives with respect to p_i.

$\Rightarrow$ Convergence in distribution (weak convergence) on Skorokhod space.

$\asymp$ Asymptotic proportionality up to dimensionless constants depending on fixed parameters (geometry, stiffness).

Appendix P: A Pedagogical Guide to the Derivation

P.0 Narrative Overview: From Field Alignment to Born Probabilities

This appendix provides a pedagogical overview of the derivation of the Born rule in Chronon Field Theory (ChFT), with an emphasis on the key ideas, probabilistic tools, and logical flow. Readers may wish to begin with this section to orient themselves before working through the formal results in detail.

Initial Setup and Physical Picture.

The measurement process in CFT begins with a microscopic chronon field Φ^μ loosely aligned across a boundary interface Γ with a macroscopic apparatus field Φ^μ_A. The apparatus is pre-aligned with a fixed future-directed, unit-norm, twist-free configuration, and the interface is partitioned into m disjoint channels $\{\Gamma_i\}$ corresponding to possible outcomes. The local alignment between Φ and Φ_A across each channel determines a scalar score S_i, which is then normalized to yield a probability-like overlap coordinate:

$$p_i(0) = \frac{S_i(\Phi)}{\sum_j S_j(\Phi)}.$$

This defines the initial vector $p(0) \in \Delta_{m-1}$, the *outcome simplex*, which encodes how strongly the chronon field initially aligns with each outcome channel.

 doi:10.20944/preprints202508.2056.v1

Why $p(0)$ matters.

The initial overlaps $p(0)$ play the role of effective amplitude squares $|c_i|^2$. They capture all physically accessible information about the prepared state relevant to measurement outcomes, in a manner consistent with the apparatus geometry and coarse–graining; they serve as the *initial condition* for the stochastic process $p(t)$, whose evolution determines the measurement result. Conceptually, this highlights a shift from the textbook picture: the measurement is not a collapse of the system into one of its own eigenstates, but stochastic absorption of the system field into apparatus eigen–domains. Since apparatus domains are engineered to correspond to the system's eigenbasis, there is no contradiction with the standard account; rather, CFT provides a deeper dynamical explanation of why those eigenstates appear as possible outcomes.

From Stochastic Dynamics to Absorption.

The dynamics of $p(t)$ arises from a noisy alignment process—specifically, a stochastic gradient flow for Φ coupled to the apparatus across Γ. Under a hydrodynamic scaling limit, this yields a diffusion process on Δ_{m-1} governed by a neutral (zero-drift) Wright–Fisher-type stochastic differential equation. This process has the following properties:

- It starts at $p(0)$;
- Each coordinate $p_i(t)$ is a bounded martingale;
- The process is almost surely absorbed at one of the vertices e_i (i.e., $p(\tau) = e_i$ for some i);
- Absorption is irreversible and corresponds to a definite measurement outcome.

Deriving the Born Rule.

Since each $p_i(t)$ is a martingale up to the absorption time τ, the optional stopping theorem applies:

$$\mathbb{E}[p_i(\tau)] = \mathbb{E}[p_i(0)] = p_i(0).$$

But $p_i(\tau)$ is the indicator function for outcome i, so this expectation is exactly the probability of observing i:

$$\mathbb{P}(p(\tau) = e_i) = p_i(0).$$

Thus, the Born rule emerges.

P.1 What the Born Rule Says (and How We Will Phrase It)

Statement. If a system is prepared in state $|\psi\rangle$ and measured in an orthonormal basis $\{|a_i\rangle\}_{i=1}^m$, the probability of outcome a_i is

$$\Pr(a_i \mid \psi) \;=\; |\langle a_i, \psi\rangle|^2. \tag{A59}$$

Interface phrasing. In our setup, the apparatus interface Γ is partitioned into m disjoint *channels* $\{\Gamma_i\}$ (distinct pointer regions). We form *alignment overlaps* $p_i \in [0,1]$ that sum to 1, so the vector $p = (p_1, \ldots, p_m)$ lies on the outcome simplex

$$\Delta^{m-1} \;=\; \Big\{ p \in [0,1]^m : \sum_{i=1}^m p_i = 1 \Big\}.$$

The target is to show that *single–shot* outcome probabilities equal the initial overlaps:

$$\Pr(\text{absorb at channel } i) \;=\; p_i(0) \;\equiv\; |\langle a_i, \psi\rangle|^2. \tag{A60}$$

Illustration: See Figure A4, diagram of the simplex Δ^{m-1} for $m = 3$ with a point $p(0)$ and absorbing vertices:

 doi:10.20944/preprints202508.2056.v1

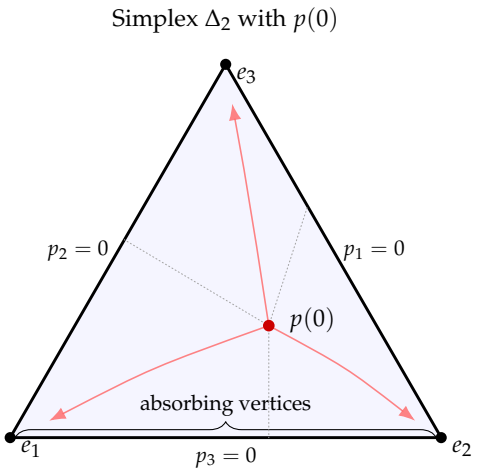

Figure A4. Simplex Δ_2 for $m = 3$. Vertices e_1, e_2, e_3 are absorbing; $p(0)$ (red) marks an initial overlap vector. Dotted guides indicate barycentric geometry; faint arrows suggest possible neutral diffusion paths toward vertices.

P.2 Why Derive It Rather Than Assume It?

- **Foundational clarity.** We seek a dynamics–based route to probabilities, avoiding postulates.
- **Device–level parameters.** The diffusion intensity and timescales are tied to measurable interface properties (coupling, temperature).
- **Robustness.** Small asymmetries or imperfections appear as small drifts/covariance perturbations whose effects can be bounded.

High–level roadmap. (i) boundary alignment $\Rightarrow$ stochastic overlap dynamics $p(t)$ on Δ^{m-1}; (ii) under symmetry and detailed balance, each coordinate $p_i(t)$ has *zero drift* (is a martingale); (iii) absorption at vertices gives outcome probabilities by optional stopping.

P.3 Chronons, overlaps, and noise: the physical picture

Chronon alignment. A microscopic field in a boundary layer near Γ tends to align with the stabilized apparatus field. Thermal/environmental noise at the boundary shakes this alignment.

- **Overlaps p_i.** Spatially averaged alignment "strengths" over each channel Γ_i, normalized to sum to 1.
- **Neutral fluctuations.** With symmetric channels and detailed balance, fluctuations are unbiased among channels: no preferred direction on Δ^{m-1}.
- **Absorption.** Once one channel dominates (all weight at a vertex of Δ^{m-1}), the process is effectively locked in: a definite outcome.

Therefore, the coarse–grained dynamics is a *neutral diffusion* on Δ^{m-1} with absorbing vertices.

In the following *Illustration*, Figure A5, the boundary layer of the apparatus region interface Γ splits into channels, with arrows showing alignment and noise:

Preprints.org (www.preprints.org) | NOT PEER-REVIEWED | Posted: 28 August 2025 doi:10.20944/preprints202508.2056.v1

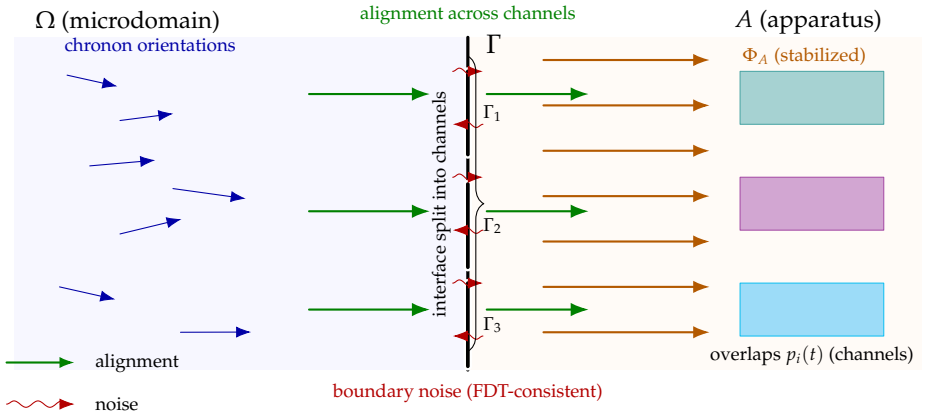

Figure A5. Boundary layer. The microdomain Ω (left) aligns with the apparatus field in A (right) through the interface Γ, which is partitioned into channels $\Gamma_1, \Gamma_2, \Gamma_3$. Solid green arrows indicate alignment flow across the interface; wavy red arrows depict boundary noise. Bars on the apparatus side schematically represent overlap observables $p_i(t)$.

P.4 The two–outcome case ($m = 2$): martingale $\Rightarrow$ Born probabilities

Let $m = 2$ and write $p(t) \in [0,1]$ for the weight of channel 1 (so channel 2 has $1 - p$). The neutral diffusion on the 1–simplex takes the canonical form

$$\mathrm{d}p(t) \;=\; \sqrt{\alpha\, p(t)\big(1 - p(t)\big)}\;\mathrm{d}W_t, \qquad \text{(no drift)} \tag{A61}$$

where $\alpha > 0$ is a diffusion intensity set by boundary fluctuations and W_t is standard Brownian motion.

Key facts (intuition, no heavy measure theory needed).

1. **Martingale property.** Since there is no drift term in (A61), the conditional expectation stays constant:
$$\mathbb{E}[\, p(t) \mid \mathcal{F}_s \,] = p(s), \quad 0 \le s \le t.$$
2. **Absorption (fixation).** The endpoints $\{0,1\}$ are absorbing; with probability 1, $p(t)$ hits $\{0,1\}$ in finite time (no "hovering" forever in the open interval).
3. **Optional stopping.** Let τ be the first hitting time of $\{0,1\}$. For bounded martingales like $p(t)$, the optional stopping theorem gives
$$\mathbb{E}[\, p(\tau)\,] \;=\; \mathbb{E}[\, p(0)\,] \;=\; p(0).$$
But $p(\tau) \in \{0,1\}$, so $\mathbb{E}[\, p(\tau)\,] = \Pr(p(\tau) = 1) \cdot 1 + \Pr(p(\tau) = 0) \cdot 0 = \Pr(\text{channel } 1)$.

Conclusion (two–outcome Born rule).

$$\Pr(\text{absorb at channel } 1) \;=\; p(0), \qquad \Pr(\text{absorb at channel } 2) \;=\; 1 - p(0). \tag{A62}$$

Identifying $p(0) = |\langle a_1, \psi\rangle|^2$ matches the Born rule.

Illustration: 1D sketch of $p(t)$ as a random path starting at $p(0)$ and hitting 0 or 1 (See Figure A6):

 doi:10.20944/preprints202508.2056.v1

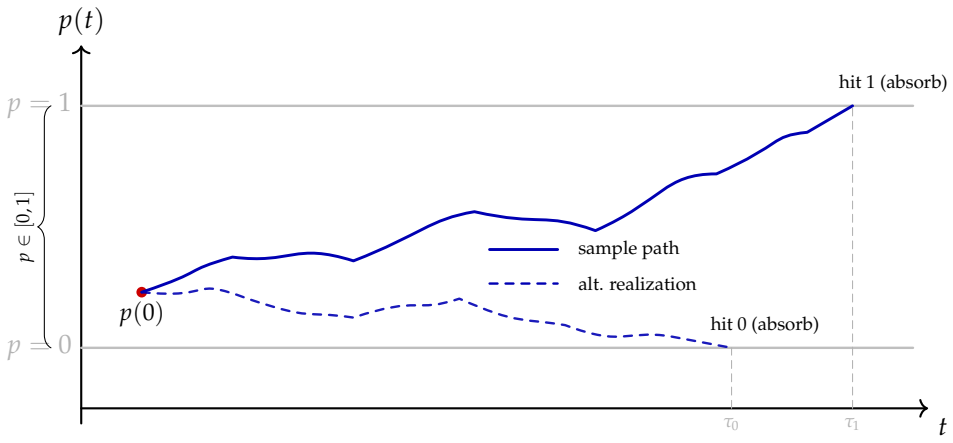

Figure A6. One-dimensional sketch of the overlap coordinate $p(t)$ under neutral diffusion. The process starts at $p(0)$ (red) and, depending on noise, is absorbed at $p = 1$ (solid path, time τ_1) or at $p = 0$ (dashed path, time τ_0).

P.5 From Two Outcomes to Many: Simplex Diffusion, Frequencies, and Robustness

Many outcomes. For $m \geq 2$, the overlap vector $p(t) \in \Delta^{m-1}$ follows a neutral Wright–Fisher diffusion:

$$\mathrm{d}p_i(t) \;=\; \sum_{j=1}^{m} \sigma_{ij}(p(t))\,\mathrm{d}W_j(t), \qquad \mathrm{Cov}\big(\mathrm{d}p_i, \mathrm{d}p_j\big) \;=\; \alpha\big(\delta_{ij}p_i - p_i p_j\big)\,\mathrm{d}t, \tag{A63}$$

with absorbing vertices e_i (pure channels). Each coordinate $p_i(t)$ is a bounded martingale, so the same optional–stopping logic gives

$$\Pr\big(p(\tau) = e_i\big) \;=\; p_i(0)\,. \tag{A64}$$

Repeated trials & frequencies. Independent repeats (or sufficiently mixing repeats) produce empirical frequencies $\hat{f}$ that concentrate at $p(0)$ with exponentially small tails; the large–deviation rate is the relative entropy $I(q) = \sum_i q_i \log\big(q_i / p_i(0)\big)$.

Robustness. Small asymmetries or finite–temperature effects appear as a small drift $b^*(p)$ or a small perturbation of the covariance. Deviations in absorption probabilities can be bounded proportionally to these small parameters (qualitative statement).

Illustration: 2D simplex ($m = 3$) with sample diffusion paths from $p(0)$ to vertices (See Figure A7):

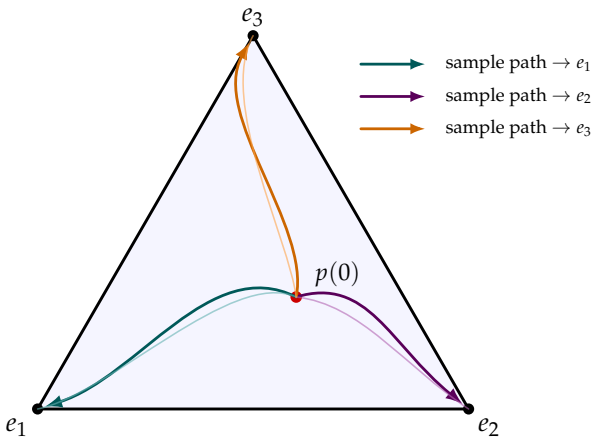

Figure A7. Diffusion on the simplex Δ_2 starting at $p(0)$ (red). Sample paths (colored) terminate at absorbing vertices e_1, e_2, e_3, illustrating fixation to a single outcome.

 doi:10.20944/preprints202508.2056.v1

P.6 Martingales and Optional Stopping

A stochastic process $(M_t)_{t\geq 0}$ adapted to a filtration $\mathcal{F}_t$ is called a *martingale* if

$$\mathbb{E}[M_{t+s} \mid \mathcal{F}_t] = M_t, \qquad \forall s \geq 0,$$

and $\mathbb{E}[|M_t|] < \infty$. Intuitively, martingales have no drift: their conditional expectation at a later time is the current value.

A key tool in our derivation is the *optional stopping theorem* (OST), which provides conditions under which $\mathbb{E}[M_\tau] = \mathbb{E}[M_0]$ for a random stopping time τ. For bounded martingales, OST holds for any bounded stopping time. In our context, the coordinate processes $p_i(t)$ on the simplex are martingales that almost surely hit one of the absorbing vertices. OST then identifies the absorption probabilities with the initial values $p_i(0)$. See Figure A8 for an illustration.

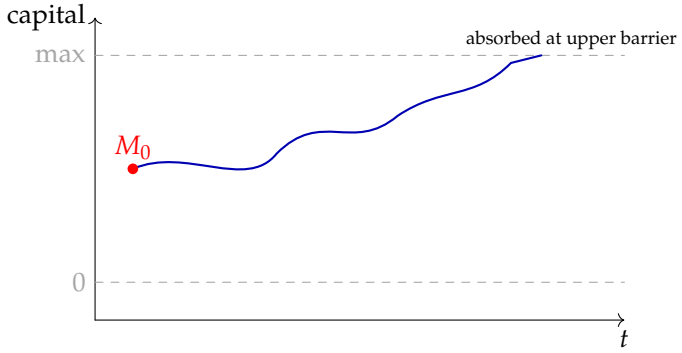

Figure A8. A martingale path (blue) stopped at a random time τ. Optional stopping ensures $\mathbb{E}[M_\tau] = \mathbb{E}[M_0]$.

P.7 Wright–Fisher Diffusions on the Simplex

The Wright–Fisher diffusion is a canonical stochastic model for allele frequencies in a population of fixed size. For m types, the state space is the simplex

$$\Delta_{m-1} = \{p \in \mathbb{R}^m : p_i \geq 0, \sum_{i=1}^{m} p_i = 1\}.$$

In the diffusion limit of large populations, the process $p(t)$ evolves according to the Itô SDE

$$dp_i(t) \;=\; \sum_{j=1}^{m} \sqrt{p_i(t)(\delta_{ij} - p_j(t))}\, dW_{ij}(t),$$

with correlated Brownian motions $W_{ij}(t)$. The vertices of Δ_{m-1} are absorbing: once the process hits a vertex (fixation of a single type), it remains there. The absorption probabilities equal the initial proportions, echoing the martingale property.

In our apparatus model, the overlap coordinates $p_i(t)$ follow an analogous diffusion with absorbing vertices, making the Wright–Fisher process a natural reference point. See Figure A9 for an illustration.

 doi:10.20944/preprints202508.2056.v1

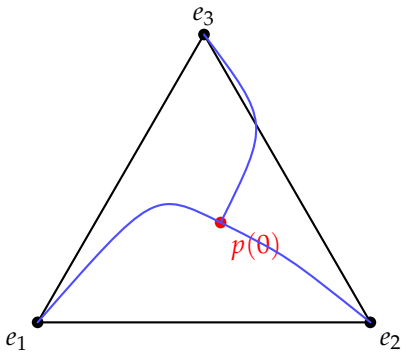

Figure A9. Wright–Fisher diffusion on Δ_2: starting from $p(0)$, sample paths eventually fixate at one absorbing vertex.

P.8 Relative Entropy and Sanov's Theorem

Relative entropy (or Kullback–Leibler divergence) between two probability distributions q and p on a finite alphabet is

$$D(q\|p) = \sum_i q_i \log \frac{q_i}{p_i}.$$

It is always nonnegative and vanishes iff $q = p$.

Sanov's theorem describes the large deviations of empirical measures from i.i.d. samples. If $X_1, \ldots, X_n$ are drawn i.i.d. from distribution p, and L_n denotes the empirical distribution, then

$$\Pr(L_n \approx q) \asymp \exp\big(-n\, D(q\|p)\big),$$

in the sense of large-deviation asymptotics. Thus the most likely empirical frequency vector is p itself, and deviations are exponentially suppressed with rate $D(q\|p)$.

In our repeated-trial setting, Sanov's theorem explains why the empirical frequencies of outcomes concentrate near the Born vector, with relative entropy furnishing the rate function of the large-deviation principle. See Figure A10 for an illustration.

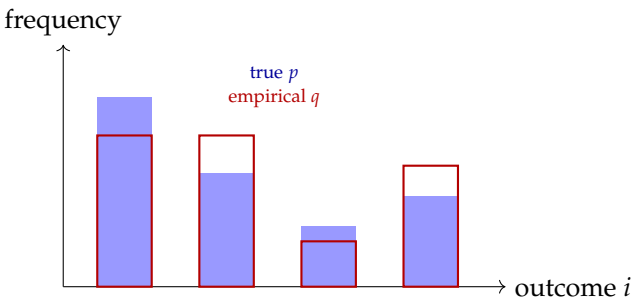

Figure A10. Sanov's theorem: the probability that empirical frequencies (red) deviate from the true distribution (blue) decays like $\exp[-nD(q\|p)]$.

Further reading pointers. For curious readers, we suggest quick primers on: (i) optional stopping for bounded martingales [93], (ii) Wright–Fisher diffusions on the simplex [27,33], and (iii) relative entropy and Sanov's theorem [16,19].

Funding: This research received no external funding

Abbreviations

The following abbreviations are used in this manuscript:

ChFT Chronon Field Theory

 doi:10.20944/preprints202508.2056.v1

References

1. D. J. Aldous. Stopping times and tightness. *Annals of Probability*, 6(2):335–340, 1978.
2. D. Bakry, I. Gentil, and M. Ledoux. *Analysis and Geometry of Markov Diffusion Operators*. Springer, 2014.
3. A. Barchielli and M. Gregoratti. *Quantum Trajectories and Measurements in Continuous Time: The Diffusive Case*. Springer, 2009.
4. A. Bassi and G. C. Ghirardi. Dynamical reduction models. *Physics Reports*, 379(5-6):257–426, 2003.
5. A. Bassi and G. C. Ghirardi. The GRW model: Past, present and future. *J. Phys. A: Math. Theor.*, 40:2919–2933, 2009.
6. A. Bassi, K. Lochan, S. Satin, T. P. Singh, and H. Ulbricht. Models of wave-function collapse, underlying theories, and experimental tests. *Rev. Mod. Phys.*, 85(2):471–527, 2013.
7. P. Billingsley. *Probability and Measure*, 3rd ed. Wiley, 1995.
8. P. Billingsley. *Convergence of Probability Measures*, 2nd ed. Wiley, 1999.
9. H. Brezis, *Functional Analysis, Sobolev Spaces and Partial Differential Equations*, Springer, 2010.
10. W. Bryc and A. Dembo. Large deviations for quadratic functionals of stationary Gaussian processes. *J. Theor. Probab.*, 9(4):725–752, 1996.
11. P. Busch. Is the quantum state (an) observable? In *Quantum Structures and the Nature of Reality*, pp. 61–70. Springer, 1999.
12. P. Busch, P. Lahti, and P. Mittelstaedt. *The Quantum Theory of Measurement*, 2nd ed. Springer, 1996.
13. C. M. Caves, C. A. Fuchs, and R. Schack. Quantum probabilities as Bayesian probabilities. *Phys. Rev. A*, 65:022305, 2002.
14. D. Chandler. *Introduction to Modern Statistical Mechanics*. Oxford University Press, 1987.
15. B. S. Cirel'son. Quantum generalizations of Bell's inequality. *Lett. Math. Phys.*, 4(2):93–100, 1980.
16. T. M. Cover and J. A. Thomas. *Elements of Information Theory*, 2nd ed. Wiley, 2006.
17. G. Da Prato and J. Zabczyk. *Stochastic Equations in Infinite Dimensions*. Cambridge University Press, 1992.
18. J. Dedecker and F. Merlevède. Necessary and sufficient conditions for the conditional central limit theorem. *Annals of Probability*, 34(3):1044–1051, 2006.
19. A. Dembo and O. Zeitouni. *Large Deviations Techniques and Applications*, 2nd ed. Springer, 1998.
20. D. Deutsch. Quantum theory of probability and decisions. *Proc. R. Soc. Lond. A*, 455:3129–3137, 1999.
21. L. Diósi. A universal master equation for the gravitational violation of quantum mechanics. *Phys. Lett. A*, 120(8):377–381, 1987.
22. L. Diósi. Continuous quantum measurement and Itô formalism. *Phys. Lett. A*, 129(8-9):419–423, 1988.
23. R. L. Dobrushin. The description of a random field by means of conditional probabilities and conditions of its regularity. *Theory of Probability and Its Applications*, 13(2):197–224, 1968.
24. H.-O. Georgii. *Gibbs Measures and Phase Transitions*, 2nd ed. de Gruyter, 2011.
25. F. den Hollander. *Large Deviations*. American Mathematical Society, 2000.
26. J. L. Doob. *Stochastic Processes*. Wiley, 1953.
27. R. Durrett. *Probability Models for DNA Sequence Evolution*, 2nd ed. Springer, 2008.
28. R. Durrett. *Probability: Theory and Examples*, 5th ed. Cambridge University Press, 2019.
29. R. S. Ellis. *Entropy, Large Deviations, and Statistical Mechanics*. Springer, 1985.
30. C. L. Epstein and R. Mazzeo. Wright–Fisher diffusion in one dimension. *SIAM J. Math. Anal.*, 45(2):625–652, 2013.
31. S. N. Ethier and T. G. Kurtz. *Markov Processes: Characterization and Convergence*. Wiley, 1986.
32. L. C. Evans, *Partial Differential Equations*, 2nd ed., Graduate Studies in Mathematics, Vol. 19, American Mathematical Society, 2010.
33. W. J. Ewens. *Mathematical Population Genetics I: Theoretical Introduction*, 2nd ed. Springer, 2004.
34. C. A. Fuchs, N. D. Mermin, and R. Schack. An introduction to QBism with an application to the locality of quantum mechanics. *Am. J. Phys.*, 82(8):749–754, 2014.
35. M. Fukushima, Y. Oshima, and M. Takeda. *Dirichlet Forms and Symmetric Markov Processes*, 2nd ed. de Gruyter, 2011.
36. D. A. Freedman. On tail probabilities for martingales. *Annals of Probability*, 3(1):100–118, 1975.
37. M. I. Freidlin and A. D. Wentzell. *Random Perturbations of Dynamical Systems*, 3rd ed. Springer, 2012.
38. M. Gell-Mann and J. B. Hartle. Quantum mechanics in the light of quantum cosmology. In *Complexity, Entropy and the Physics of Information*, 1990.
39. G. C. Ghirardi, A. Rimini, and T. Weber. Unified dynamics for microscopic and macroscopic systems. *Phys. Rev. D*, 34(2):470–491, 1986.

 doi:10.20944/preprints202508.2056.v1

40. N. Gisin. Quantum measurements and stochastic processes. *Phys. Rev. Lett.*, 52:1657–1660, 1984.
41. A. M. Gleason. Measures on the closed subspaces of a Hilbert space. *J. Math. Mech.*, 6(6):885–893, 1957.
42. M. S. Green. Markoff random processes and the statistical mechanics of time-dependent phenomena. II. *J. Chem. Phys.*, 22:398–413, 1954. R. Kubo. Statistical-mechanical theory of irreversible processes. I. *J. Phys. Soc. Japan*, 12(6):570–586, 1957.
43. R. C. Griffiths. The expected time to absorption in neutral stochastic processes. *Advances in Applied Probability*, 11(3):486–501, 1979.
44. M. Grmela and H. C. Öttinger. Dynamics and thermodynamics of complex fluids. I. *Physical Review E*, 56(6):6620–6632, 1997.
45. M. Hairer, *An Introduction to Stochastic PDEs*, arXiv:0907.4178, 2011.
46. N. Harrigan and R. W. Spekkens. Einstein, incompleteness, and the epistemic view of quantum states. *Found. Phys.*, 40:125–157, 2010.
47. S. W. Hawking and G. F. R. Ellis, *The Large Scale Structure of Space-Time*, Cambridge University Press, 1973.
48. W. Hoeffding. Probability inequalities for sums of bounded random variables. *J. Am. Stat. Assoc.*, 58(301):13–30, 1963.
49. R. Holley and D. Stroock. Logarithmic Sobolev inequalities and stochastic Ising models. *Communications in Mathematical Physics*, 115(3):553–569, 1988.
50. J. Jacod and A. N. Shiryaev. *Limit Theorems for Stochastic Processes*, 2nd ed. Springer, 2003.
51. E. Joos et al. *Decoherence and the Appearance of a Classical World in Quantum Theory*, 2nd ed. Springer, 2003.
52. O. Kallenberg. *Foundations of Modern Probability*, 2nd ed. Springer, 2002.
53. I. Karatzas and S. E. Shreve. *Brownian Motion and Stochastic Calculus*, 2nd ed. Springer, 1991.
54. S. Karlin and H. M. Taylor. *A Second Course in Stochastic Processes*. Academic Press, 1981.
55. C. Kipnis and C. Landim. *Scaling Limits of Interacting Particle Systems*. Springer, 1999.
56. C. Kipnis and S. R. S. Varadhan. Central limit theorem for additive functionals of reversible Markov processes. *Communications in Mathematical Physics*, 104(1):1–19, 1986.
57. P. E. Kloeden and E. Platen. *Numerical Solution of Stochastic Differential Equations*. Springer, 1992.
58. T. Komorowski, C. Landim, and S. Olla. *Fluctuations in Markov Processes: Time Symmetry and Martingale Approximation*. Springer, 2012.
59. R. Kubo. The fluctuation–dissipation theorem. *Reports on Progress in Physics*, 29(1):255–284, 1966.
60. T. G. Kurtz and P. Protter. Weak limit theorems for stochastic integrals and stochastic differential equations. *Annals of Probability*, 19(3):1035–1070, 1991.
61. T. G. Kurtz. Averaging for martingale problems. In *Stochastic Analysis*, pp. 186–209. Academic Press, 1992.
62. D. A. Levin and Y. Peres. *Markov Chains and Mixing Times*, 2nd ed. AMS, 2017.
63. B. Li. Emergence and Exclusivity of Lorentzian Signature and Unit–Norm Time from Random Chronon Dynamics. Zenodo, https://doi.org/10.5281/zenodo.16922773
64. R. S. Liptser and A. N. Shiryayev. *Statistics of Random Processes I: General Theory*. Springer, 1977.
65. C. Maes and K. Netočný. Time-reversal and entropy. *Journal of Statistical Physics*, 110(1):269–310, 2003.
66. S. P. Meyn and R. L. Tweedie, *Markov Chains and Stochastic Stability*, 2nd ed. Cambridge University Press, 2009.
67. H. Mori. Transport, collective motion, and Brownian motion. *Progress of Theoretical Physics*, 33(3):423–455, 1965.
68. M. A. Naimark. Spectral functions of a symmetric operator. *Izvestiya Akad. Nauk SSSR Ser. Mat.*, 4:277–318, 1940.
69. E. Nelson. Derivation of the Schrödinger equation from Newtonian mechanics. *Phys. Rev.*, 150(4):1079–1085, 1966.
70. A. Dembo and O. Zeitouni. *Large Deviations Techniques and Applications*, 2nd ed. Springer, 1998.
71. S. Orey and S. Pelikan. Large deviations for stationary processes. *Annals of Probability*, 17(4):1481–1495, 1989.
72. H. C. Öttinger. *Beyond Equilibrium Thermodynamics*. Wiley, 2005.
73. G. C. Papanicolaou and W. Kohler, Asymptotic theory of mixing stochastic ordinary differential equations, *Communications on Pure and Applied Mathematics*, 27(5):641–668, 1974.
74. G. A. Pavliotis. *Stochastic Processes and Applications*. Springer, 2014.
75. G. A. Pavliotis and A. M. Stuart. *Multiscale Methods: Averaging and Homogenization*. Springer, 2008.
76. R. Penrose. On gravity's role in quantum state reduction. *Gen. Relativ. Gravit.*, 28(5):581–600, 1996.
77. A. Peres. Neumark's theorem and quantum inseparability. *Foundations of Physics*, 20:1441–1453, 1990.
78. G. A. Pavliotis and A. M. Stuart. *Multiscale Methods: Averaging and Homogenization*. Springer, 2008.

 doi:10.20944/preprints202508.2056.v1

79. R. Rebolledo. Central limit theorems for local martingales. *Zeitschrift für Wahrscheinlichkeitstheorie und Verwandte Gebiete*, 51:269–286, 1980.
80. J. Jacod and A. N. Shiryaev. *Limit Theorems for Stochastic Processes*, 2nd ed. Springer, 2003.
81. D. Revuz and M. Yor. *Continuous Martingales and Brownian Motion*, 3rd ed. Springer, 1999.
82. I. N. Sanov. On the probability of large deviations of random variables. *Mat. Sb.*, 42(84):11–44, 1957.
83. R. D. Skeel and J. Izaguirre. An impulse integrator for Langevin dynamics. *Molecular Physics*, 100(24):3885–3891, 2002.
84. R. W. Spekkens. Evidence for the epistemic view of quantum states: A toy theory. *Phys. Rev. A*, 75:032110, 2007.
85. H. Spohn, *Large Scale Dynamics of Interacting Particles*, Springer, 1991.
86. D. W. Stroock and S. R. S. Varadhan, *Multidimensional Diffusion Processes*, Springer, 1979.
87. S. R. S. Varadhan. *Large Deviations and Applications*. SIAM, 1984.
88. S. R. S. Varadhan. *Stochastic Processes*. Courant Lecture Notes in Mathematics, vol. 16, AMS/CIMS, 2007.
89. R. Vershynin. *High-Dimensional Probability: An Introduction with Applications in Data Science*. Cambridge University Press, 2018.
90. J. von Neumann. *Mathematical Foundations of Quantum Mechanics*. Princeton University Press, 1955.
91. D. Wallace. *The Emergent Multiverse: Quantum Theory According to the Everett Interpretation*. Oxford University Press, 2012.
92. W. Whitt. *Stochastic-Process Limits*. Springer, 2002.
93. D. Williams. *Probability with Martingales*. Cambridge University Press, 1991.
94. H. M. Wiseman and G. J. Milburn. *Quantum Measurement and Control*. Cambridge University Press, 2009.
95. T. Yamada and S. Watanabe. On the uniqueness of solutions of stochastic differential equations. *Journal of Mathematics of Kyoto University*, 11(1):155–167, 1971.
96. B. Zegarliński. Logarithmic Sobolev inequalities for Gibbs measures. *Probability Theory and Related Fields*, 89(2):199–213, 1991.
97. W. H. Zurek. Environment-induced superselection rules. *Phys. Rev. D*, 26(8):1862–1880, 1982.
98. W. H. Zurek. Decoherence, einselection, and the quantum origins of the classical. *Rev. Mod. Phys.*, 75(3):715–775, 2003.
99. W. H. Zurek. Probabilities from entanglement, Born's rule from envariance. *Phys. Rev. A*, 71:052105, 2005.
100. R. Zwanzig. Memory effects in irreversible thermodynamics. *Journal of Chemical Physics*, 33(5):1338–1341, 1961.